THE JOURNAL OF COMPARATIVE NEUROLOGY 254:425-459 (1986)

Embryogenesis of Arborization Pattern and Topography of Individual Axons in N. Laminaris of the Chicken Brain Stem

STEVEN R. YOUNG AND EDWIN W RUBEL
Departments of Otolaryngology and Physiology (E.W R.), and Neuroscience Program (S.R.Y.,E.W R.), University of Virginia Medical Center, Charlottesville, Virginia 22908

ABSTRACT

This study examined the development of individual axon terminal fields in n. laminaris (NL) of the chicken brainstem. In their mature form axons from the nucleus magnocellularis (NM), second-order auditory neurons in the chicken brainstem, project bilaterally onto the NL. Axons from the ipsilateral and contralateral NM neurons form spatially segregated, elongated arbors in the dorsal and ventral neuropil of NL, respectively. The long axes of these arbors correspond to physiologically defined isofrequency bands. To assess the development of this stereotyped arborization pattern, 6–17-day embryonic chicken brain stems were maintained *in vitro* while injecting horseradish peroxidase into small groups of axons. Three-dimensional reconstructions were made from serial sections and projected onto a cartesian plane for quantitative analyses.

At embryonic day 6 (E6), the ventral axons already course beneath the recently migrated NL neurons. The arrival of the dorsal NM axon branches is delayed and their paths are indirect. They first loop dorsally into the the ventricular layer, where they seem to make specific connections with migrating NL neurons and use these as guides to their appropriate positions in the NL.

During the period from E9 to E17 the dorsal and ventral terminal fields become similar, each adopting properties of the other's initial pattern. The dorsal terminal fields extend to form bands similar to the early ventral terminal fields, while the ventral terminal fields narrow and appear to shift position in order to achieve the tonotopic specificity characteristic of the early dorsal terminal fields.

The results show that a complex, mature pattern of neuronal connections can be formed during development by the combination and reorganization of two simple patterns—each shaped, in turn, by its respective axonal trajectory.

Key words: synapse reorganization, auditory, development, axon growth

How do growing nerve cells find and select the appropriate targets among all the other cells within their reach? Evidently, most connections in the developing embryo initially are rather precise but become further constrained during the early period of electrical activity. For example, horseradish peroxidase injections into the chick hindlimb and spinal cord indicate that most axons find their routes on the basis of pathway constraints and local cues at decision points (Tosney and Landmesser, '85a,b). Intracellular dye injections into embryonic grasshopper neurons show that growth cone filopodia can identify "guidepost" cells

Accepted June 17, 1986.

Address reprint requests to Edwin W Rubel, Department of Otolaryngology, BB1167, Health Sciences Building, RL-30, University of Washington, Seattle, WA 98195.

Preliminary results were presented previously (Young and Rubel, '84).

Steve Young's present address is Department of Physiology and Biophysics, R-430, University of Miami Medical School, P. O. Box 016430, Miami, FL 33101.

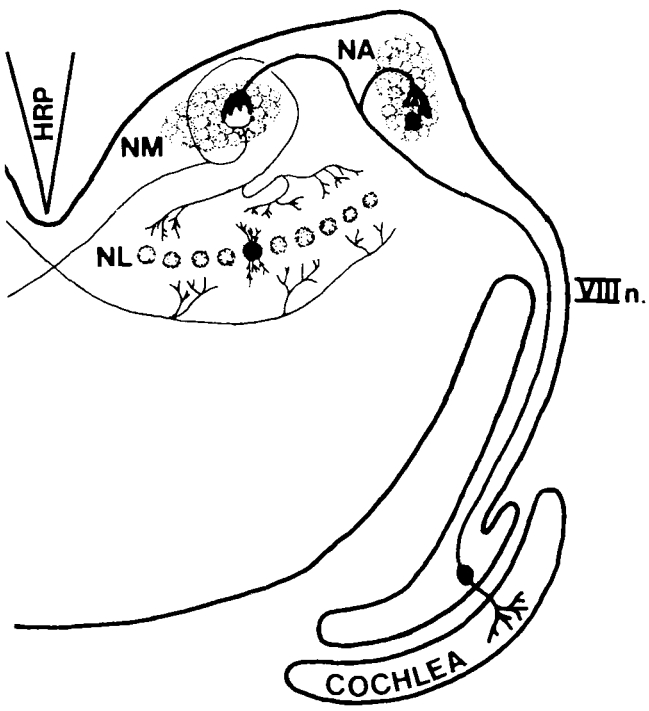

Fig. 1. Schematic of coronal section of brainstem showing the cochlea, eighth nerve (VIII n.), n. angularis (NA), n. magnocellularis (NM), and n. laminaris (NL). Dorsal and ventral NL neuropil regions are separated by the cell body layer. The location of most of the HRP injections is indicated by the pipette at the dorsal midline.

that mark the axon's pathway (Ho and Goodman, '82; Keshishian and Bentley, '83a,b,c). In many systems, secondary reorganizations of the axons establish the final pattern of connections once the axons are within the target region (LeVay et al., '78; Lichtman and Purves, '80; Jackson and Parks, '82; Easter and Stuermer, '84; Stuermer and Easter, '84; Sretavan and Shatz, '86).

The topographic arrangement of sensory projections has offered a good criterion with which to evaluate developing connections. The topographic projection from n. magnocellularis (NM) to n. laminaris (NL) in the chick brain stem has particularly interesting properties. The NM is a second-order nucleus receiving frequency-specific auditory information from the cochlea (Fig. 1). The NL is a monolayer of neurons with segregated dorsal and ventral neuropil regions. Sound frequencies map as an ordered continuum in both NM and NL (tonotopic organization). The axis of this tonotopic organization in both NM and NL follows a line from the posterolateral (low frequencies) to the anteromedial (high frequencies) poles of the nuclei (Parks and Rubel, '75; Rubel and Parks, '75). Each NM neuron projects bilaterally to the NL, ipsilaterally to the dorsal neuropil and cell bodies, and contralaterally to the ventral NL neuropil and cell bodies. Each collateral forms a narrow terminal arborization arranged perpendicularly to the axis of the tonotopic organization (Young and Rubel, '83). In the adult, this termination pattern is similar in the dorsal and the ventral neuropil of NL, and the tonotopic maps produced by the two NM projections to the NL are in register. This system provides the opportunity to study how axons following entirely separate pathways are able to produce identical tonotopic maps in their target.

Horseradish peroxidase (HRP) injections of small numbers of axons and serial section reconstructions of individual axonal arborizations were used to study the NM to NL projection in embryos ranging from 6 days of incubation through 1 month posthatch. In addition to the simple organization of the system (Fig. 1), several other factors aided this study. The NM axons are, by far, the predominant input to the NL (Parks et al., '83). The acellular dorsal and ventral neuropil layers can be well characterized by projecting them graphically onto a single planar surface (Rubel and Parks, '75; Smith and Rubel, '79; Young and Rubel, '83). This facilitates quantitation of NM axon terminal fields. Furthermore, background information on cell birthdates, cell death (Rubel et al., '76), dendritic development (Smith, '81), eighth nerve terminal development (Jhaveri and Morest, '82b,c), functional synaptogenesis (Jackson et al., '82), and development of hearing (Saunders, '73; Jackson and Rubel, '78; Rebillard and Rubel, '81) is available.

MATERIALS AND METHODS

Subjects

A total of 269 chicks from embryonic day 6 (E6) to 30 days after hatching (P30) were used. Hubbard × Hubbard or Ross Arbor Acres eggs were obtained from local breeders and incubated at 37–38°C in a forced-draft incubator. Embryos were staged at the time of HRP injection according to Hamburger and Hamilton ('51). Days of embryonic age referred to in this paper are the ages appropriate to the Hamburger and Hamilton stages. These usually correspond to chronological age but some scatter occurs normally. Only Ross Arbor Acres embryos were used for the quantitative comparisons.

Of the total number of chicks used, some were uninjected controls of the chromagen reaction; others were used to verify the physiological viability of the preparation, and still others were processed for electron microscopic examinations that will be described in a later paper. Brains from 104 chicks with successful HRP injections were used to study the development of terminal morphology and for nonquantitative examination of the NM axons and terminal fields. The same brains provided material for the study of dendritic development in the NM and for estimates of the frequency of various aberrant axonal projections. From these 104 successful injections, 199 well-stained axonal arborizations from 23 animals were drawn and completely reconstructed. One hundred one terminal fields from 16 brains between E9 and E17 formed the material for a quantitative analysis of terminal field shape, size, and orientation. Table 1 shows how these terminal fields were distributed by age and location.

Dissection and HRP injections

The dissection was performed with the embryo immersed in cold (1–4°C) avian Tyrode's solution (139 mM NaCl, 3 mM KCl, 17 mM $NaHCO_3$, 1 mM $MgCl_2$, 3 mM $CaCl_2$, 12.2 mM dextrose, bubbled with 95% O_2, 5% CO_2). The embryo was removed from the shell and the head (or the entire embryo at early stages) was pinned in a dish coated with Sylgard (Dow-Corning). Within 1–3 minutes, the brain was exposed and the fourth ventricle was flushed with cold Tyrode's solution. The spinal cord was cut at the level of the first vertebra, and the forebrain, midbrain, and cerebel-

TABLE 1. Distribution of Terminal Fields in Quantitative Analysis[1]

	Age group								
	E9	E9–14					E14–17		
	(Stage 35)	35+*	36*	37*	39+*	Total	40*	43*	Total
Dorsal									
A	6	2	6	4	4	16	9	2	11
P	2	—	—	3	—	3	6	3	9
Total	8	2	6	7	4	19	15	5	20
Ventral									
A	13	1	3	9	4	17	3	6	9
P	5	—	—	4	2	6	4	—	4
Total	18	1	3	13	6	23	7	6	13

[1]The 101 terminal fields measured and compared with an ANOVA are shown as they were distributed by age group, stage, side (dorsal or ventral), and position [anterior (A) or posterior (P)].
[2]Most of our material from this period was at Hamburger and Hamilton ('51) stage 37 (E11), but single embryos at stages 35+, 36, and 39+ are also included with the E11 chicks.
*Stages.

lum were removed. The remaining cranial nerves were cut, and the brain stem was lifted from the cranium. The explant was then transferred to a plexiglas chamber, which permitted transillumination of the tissue, and the temperature was raised slowly to 32–35°C over about 90 minutes.

Auditory nuclei in chick brain stems isolated and maintained *in vitro* have been shown to continue responding to electrical stimulation of the eighth nerve for 8 hours or more (Hackett et al., '82). Thus, in early experiments on E14 to E18 embryos, placement of the injection pipette was guided by physiological responses either in the NM or in the crossed dorsal cochlear tract. However, because most of this study was carried out at stages before the entire NM becomes responsive to stimulation of the eighth nerve (E13; Jackson et al., '82), a method of visual placement of the injection pipette was developed (see below). Subsequently, physiological recordings from embryos receiving HRP injections were made only rarely.

Injection pipettes were filled with 2% horseradish peroxidase (HRP, Sigma type VI), 0.2% fast green, and 0.2 M NaCl in 0.01 M Tris buffer, pH 7.6. The pipette tip was broken to an outside diameter of 2–5 μm. Transillumination with a fiber optic light and a Leitz darkfield condenser allowed both the tip of the dye-filled pipette and the more superficial fibers of the crossed dorsal cochlear tract to be seen clearly. The pipette was lowered with a micromanipulator until the tip could be seen among the crossing NM fibers at the midline, 50–100 μm below the ependymal surface. The pipette was then tapped lightly to sever a small number of fibers. HRP was ejected by applying pressure pulses of 10–20 psi, 2.5–5 ms long, at a frequency of about 1 Hz with a Picospritzer (General Valve Corporation). A small amount of HRP was ejected in this way for 1–3 hours, and the tissue was maintained in the chamber for an additional 1–2 hours. Three to 4 hours after the injection was begun, the tissue was immersed in 37°C fixative (0.5% or 1% paraformaldehyde, 2.5% glutaraldehyde, 15 mM $MgSO_4$, and 3% sucrose in 0.12 M Na/K PO_4 buffer, pH 7.2) for 15–30 minutes, transferred to refrigerated fixative of the same composition, and left refrigerated overnight.

Histology

Fixed brainstems were blocked and washed in cold 0.12 M Na/K PO_4 buffer, pH 7.5. The tissue was embedded in 12% gelatin and kept at 4°C. Vibratome sections (40–60 μm) in the coronal plane were cut into fresh, ice-cold buffer. The sections were mounted on gelatin-subbed slides, dried, rinsed briefly in PO_4 buffer, and then treated with diaminobenzidine according to the method of Adams ('81). In later experiments, the sections were counterstained with 0.05% toluidine blue with 0.5% sodium tetraborate, rinsed thoroughly with distilled water, and dehydrated through an acetone series. Sections were cleared in xylene and coverslipped with Lipshaw neutral mounting medium.

Reconstructions

Axons were chosen for complete reconstruction on the basis of three criteria: (1) Complete filling of the axonal arborization. Incomplete filling was manifested in two ways. Staining of the axon faded out gradually with increased distance from the injection site, or the axon had a broken, segmented appearance with thin, lightly stained segments interspersed with the normal darkly stained segments. A small degree of breaking up often did not prevent reconstruction of an axon. (2) Darkness of the reaction product and contrast against the background tissue. Many cells were lightly stained throughout, as if their axons had not been made completely permeable to the HRP at the injection site. These cells were not drawn. (3) Distinguishability of the arborization from the other stained processes. In one case (Fig. 14) 14 axons were drawn and reconstructed from one nucleus. This was possible only because of the fortuitously well-spaced distribution of the stained terminal fields along the length of NL. In most cases we used preparations with fewer than six filled axons. Rarely, a heavily stained glial process prevented reconstruction of an NM axon.

Drawings of NM axons were made with a camera lucida with ×63 or ×100 planapochromatic objectives (final magnifications: ×1,000 or ×1,250). In order to place the axons with respect to the section as a whole, a series of low-power drawings was made at the same time and salient features of the tissue were marked on both series of drawings. On the high-power drawings NL was distinguished into three areas: the cell body layer, dorsal neuropil layer, and ventral neuropil layer.

Since an NM axon extended through many 50-μm sections, high-power drawings were registered by aligning the axon from section to section. This resulted in a coronal view of the entire cell collapsed over its anterior/posterior extent. The most informative view of the relationship of the terminal fields to the lane of the NL neurons, however, was not obtained in coronal drawings but by projecting the nucleus onto a plane parallel to NL (planar projections).

In brief, the planar projections were obtained by graphic rotation of the reconstructed coronal drawings, so that the NL surface could be viewed from above without regard to depth. The loss of depth information is not a severe limitation because NL is a monolayer sheet of neurons. A three-dimensional cartesian coordinate system was established that allowed rotation of the reconstructed axons by using the midline floor of the fourth ventricle as the z axis and the horizontal and midsagittal lines intersecting it within a section as x and y axes, respectively. A detailed description of this process is available elsewhere (Young, '85). It is similar to that used previously (Rubel and Parks, '75; Smith and Rubel, '79; Lippe and Rubel, '85) except that instead of using simple projections onto the horizontal plane, a tilted projection plane was chosen that minimized distortion caused by the (limited) three-dimensional curvature of NL.

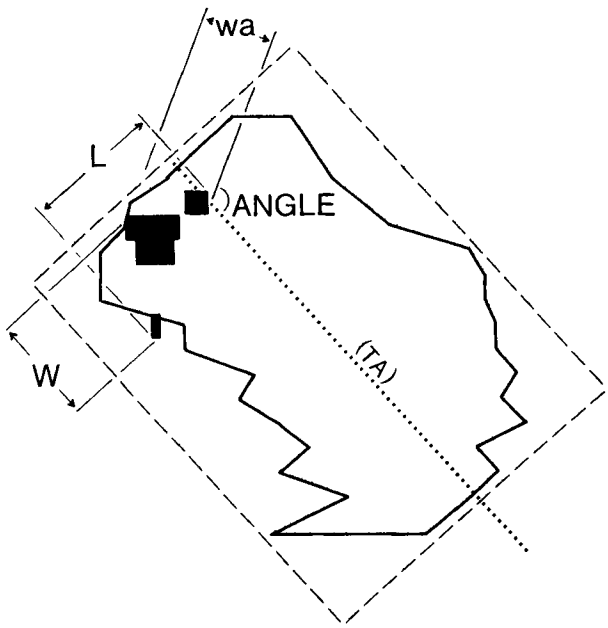

Fig. 2. Schematic of parameters used in quantitative analysis of terminal fields. Planar projection of NL (solid outline) is enclosed by dashed rectangle suggesting its idealized shape. The center line of the rectangle (dotted line) is the estimated tonotopic axis (TA) of the nucleus. The solid black rectangles show the terminal field area. This is the maximum area of NL that could be contacted by a given axon. Because of the relatively crude method of representing the terminal fields, in which terminal density and depth within the section are ignored, absolute measurements of area and width are probably greatly overestimated. The length of NL is measured along the estimated axis. L is the length of the terminal field. W is its width. wa is the minimum width of the terminal field, and ANGLE is the orientation of the terminal field at that width.

Once an optimal projection plane was chosen, the outline of NL and the position, extent, and orientation of axonal arborizations was plotted on it (Fig. 2). Plots of the actual terminal arborizations in NL were made without reference to their depth in the tissue section. Two groups of terminals were plotted separately if, in the tissue, they were separated by areas free of arborization. Thus, the rectangles on the planar projections indicate the maximum possible area of NL that could be contacted by a given NM axon. They overestimate actual terminal field size and provide little information about terminal density.

The specific criterion for plotting the width of the terminal arborization in one section was the extent of secondary branching that was within the NL neuropil. Secondary branches were not plotted as terminals until they reached the NL neuropil, nor was the main axon trunk. It should be noted that developmental changes in the morphology of the axonal arborizations could result in somewhat different characteristics being plotted at different ages (see Results).

A planar projection of the outline of NM was also drawn by using the same coordinate system and projection plane used for the ipsilateral NL. NM somata whose ipsilateral terminal fields were identified and plotted were shown on the NM planar projections.

Measurements and statistical comparisons

Quantitative analyses of terminal field shape, size, and orientation were made of 101 terminal field planar projections from E9 to E17 (Table 1). Eighteen terminal fields that were reconstructed were not included in the quantitative analysis because of breed differences, or difficulties in the reconstruction. With specific exceptions, four measurements were made of each plotted terminal field: area (A), length (L), width (W), and angle (AN). These parameters are illustrated in Figure 2. Each solid rectangle represents a cluster of endings in the NL neuropil. Since virtually all of the ventral terminal fields (53 of 54) at any age extended all the way across NL, their length was not measured. Dorsal terminal fields at E9, on the other hand, were not elongated enough to exhibit a well-defined orientation. Thus, their angle was not measured.

Area (A) is the total area of the filled rectangles in the planar projection of the terminal field. Length and width were measured with respect to an estimation of the presumptive tonotopic axis of NL (Rubel and Parks, '75; Lippe and Rubel, '85; Young, '85). Length is the maximum extent of the terminal field perpendicular to the tonotopic axis (TA in Fig. 2); width is the maximum extent parallel to the tonotopic axis. The angle (AN) of each terminal field was also measured independently of the tonotopic axis. It is the angle with respect to the estimated axis at which the minimum width of a terminal field was found with parallel rules (wa, Fig. 2). Angle measurements were used to assess the variability in terminal field orientations as well as to ensure that no systematic bias occurred in using the tonotopic axis to measure terminal field length and width.

Terminal field shape and degree of "frequency specificity" were estimated with two derivative measures. (1) The length to width ratio (L/W) of a terminal field was used as a measure of its elongation. (2) The degree of specificity of a terminal field in the frequency axis of NL was regarded as the proportion of the width of the terminal field to the overall length of NL along the tonotopic axis. W/Ln indicates the degree of specificity of a terminal field along the frequency axis of NL. Thus, a terminal field with W/Ln = 0.30 covered nearly a third of the presumptive frequency map in NL, whereas a W/Ln = 0.10 indicates coverage of only 10% of the frequency representation. This will be referred to as the width/nuclear-length ratio (W/Ln).

Developmental changes in the terminal field parameters were assessed for statistical significance by a three-way analysis of variance (ANOVA) by using age, side of NL (dorsal or ventral), and position (anterior or posterior) as variables. For the parameters L and LW, no measurements were taken from ventral terminal fields; thus a two-way ANOVA (age and position, anterior or posterior) was used. For computational purposes the data were grouped in three age groups (see Table 1): E9, E10–E13, and E14–E17. Differences between individual groups were assessed with a Newman-Keuls test (Winer, '71). Probabilities of less than .05 are reported as statistically significant.

RESULTS

Developing nucleus magnocellularis (NM) axon terminal arbors are described below in three sections covering embryonic ages E9, E11, and E14–17. A fourth section compares the qualitative and quantitative parameters of the terminal fields across age and describes how initially different dorsal and ventral terminal field patterns converge during development. The early growth of ipsilateral and contralateral NM axon branches is then described (Initial Formation of the Pathways section). Two final sections describe transient or unusual connections made by NM axons, and the development of NM dendrites.

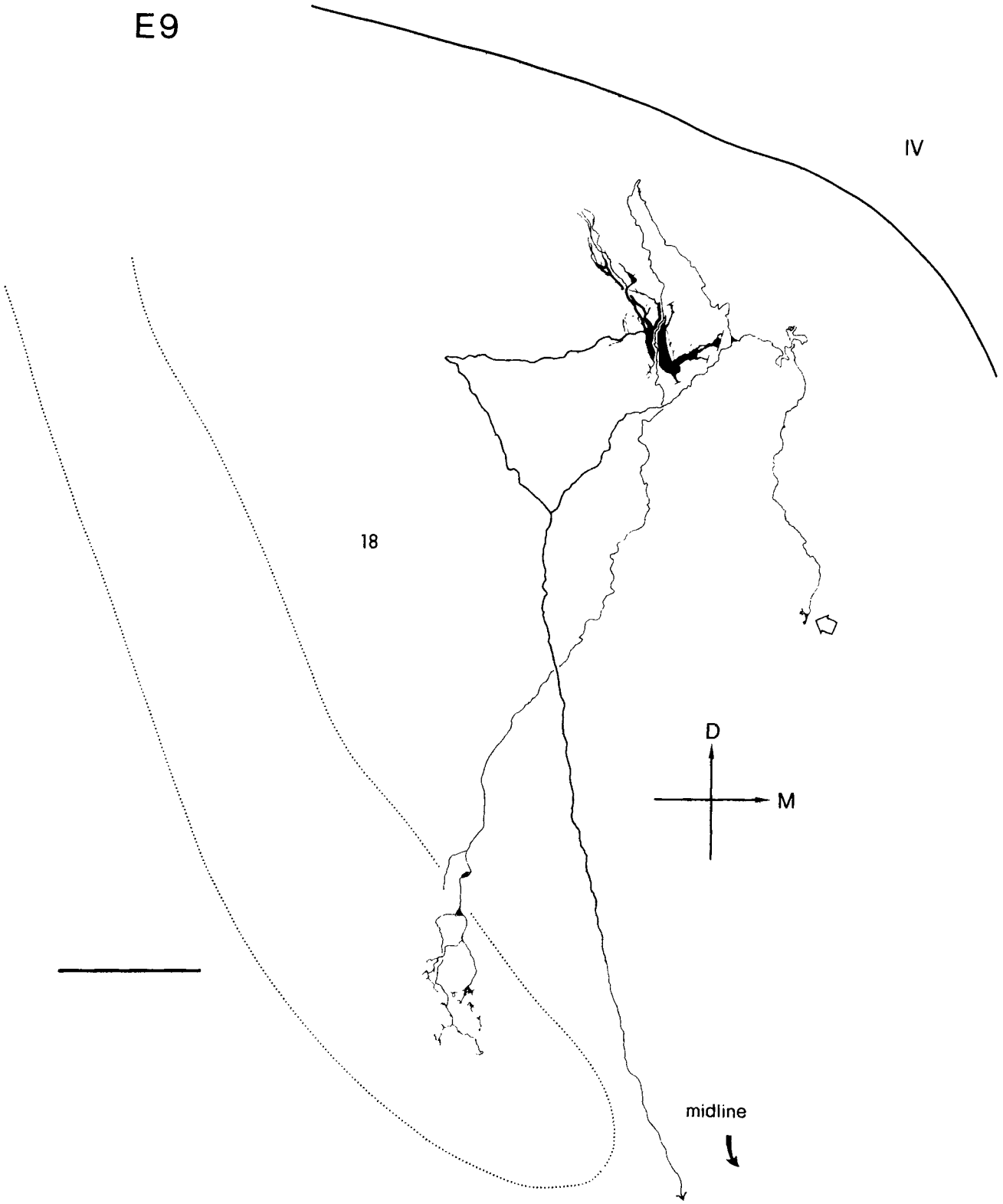

Fig. 3. Reconstruction of an HRP-filled NM neuron and axonal arborization at E9. Open arrow indicates small growth cone on an axon branch that has not reached NL. In this and all subsequent reconstructions, camera lucida drawings of several sections were combined to give a view of the axon's path and branching pattern in coronal view. The reconstructions collapse the anterior/posterior dimension. The following conventions apply to all reconstructions. The dotted line indicates NL. The solid arrow points toward the midline and the injection site. Long NM dendrites may be truncated to avoid obscuring the axon. Arrowheads at axon ends indicate that the axon continues beyond the drawing. IV is the fourth ventricle. D is dorsal; M, medial. Bar = 50 μm. This is terminal field number (TF) 18, as identified by the number beside it. The planar projection of this terminal field is shown in Figure 5B.

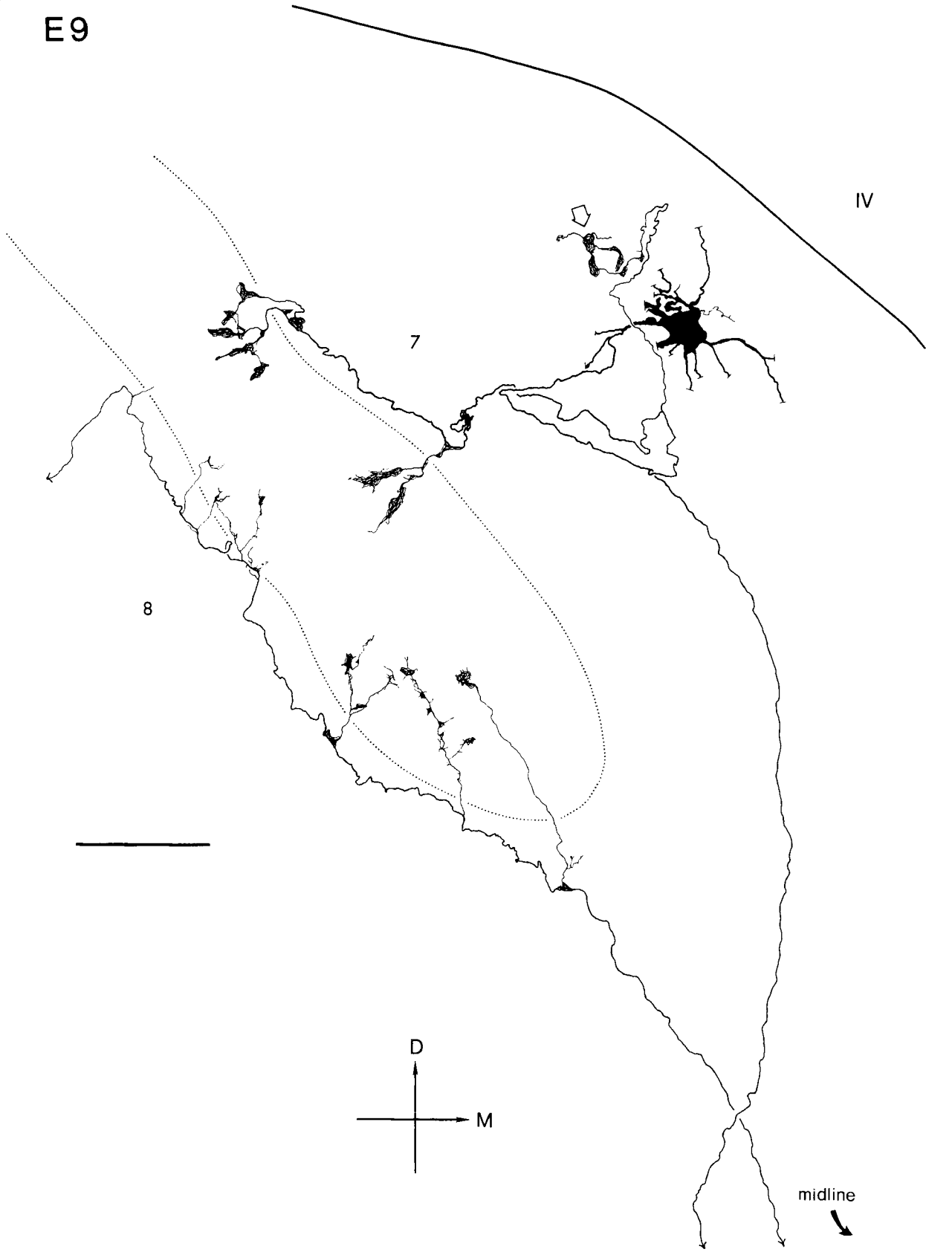

Fig. 4. Reconstruction of an E9 NM neuron with its ipsilateral dorsal arborization, and a ventral arborization from the contralateral NM (TFs 7 and 8). The open arrow indicates a large growth cone on an axon branch that has not reached NL. Conventions as in Figure 3. The medial endings of TF 7 are shown in Figure 7. Planar projections of these terminal fields are shown in Figure 5E and F.

Embryonic day 9

Branching pattern. Examination of individual NM axons at embryonic day 9 (E9) quickly revealed markedly different patterns of terminal arborization on the dorsal and ventral faces of NL. The camera lucida reconstructions in Figures 3 and 4 illustrate the E9 axonal trajectories. Figure 3 shows a stained NM neuron (terminal field No. 18 (TF 18)) backfilled from its contralateral branch at the midline. Its ipsilateral branch begins at the bifurcation ventral and lateral to the soma. It courses dorsally beyond the soma towards the ventricular surface and then turns ventrally and terminates in two sites. One termination is a simple arborization in medial NL. The second termination is a small growth cone ventromedial to the soma. Similar growth cones that have not reached NL are occasionally seen on E9 axons (Fig. 4) but are not found at E14. The loop formed by the ipsilateral branch as it courses dorsally toward the fourth ventricle and then returns toward its targets in NL is a prominent and puzzling feature of every NM axon's pathway.

Figure 4 illustrates another E9 cell body and dorsal axonal arborization (TF 7) with elaborately veiled endings in NL. A photomicrograph of the most medial endings is shown in Figure 7. Lateral to the soma, this axon has a large growth cone that has not reached NL. The loop formed by the ipsilateral branch of this axon is unusually small.

A ventral arborization (TF 8) is also shown in Figure 4. The axon's path below NL is a simple traverse from caudomedial to rostrolateral. It supports short collateral branches leading directly to arborizations in the adjacent NL neuropil. The foreshortening of this terminal field by its presentation in a coronal view can be appreciated by comparing the drawing of TF 8 in Figure 4 to its terminal field planar projection in Figure 5F.

The courses of these axons are generally similar to those taken by mature axons. In contrast, however, only the ventral terminal fields are elongated at E9. This is clearly shown in Figures 5 and 6. The dorsal terminal fields are more nearly spots than bands.

Terminal fields. Another important finding in the E9 chicks was the early positional specificity of the dorsal terminal fields. When the positions of dorsal terminal fields in NL are compared to the positions of their cell bodies in the ipsilateral NM, a general correspondence is evident. Anterior cell bodies have terminal fields in anterior NL; medial or lateral somata also have correspondingly placed terminal fields (Figs. 5,6). This is consistent with Rubel and Parks' ('75) finding of similarly oriented tonotopic axes in NM and NL. At E9, NM neurons are not activated by eighth nerve stimulation and thus tonotopy cannot be assessed physiologically. Nevertheless, if a presumptive tonotopic axis is estimated by extrapolation from older embryos (see Fig. 2), then the positions of the dorsal terminal fields along this axis in NL are similar to their cell body positions in NM. Unexpectedly, cell body and terminal field positions are in correspondence perpendicular to the tonotopic axis as well as along it. Thus, in the early projection of NM onto the ipsilateral NL there are specific positional relationships between NM cells and the NL neurons even within a presumptive isofrequency band (their mature target region). Positional specificity in this dimension can no longer be seen once the dorsal terminal fields have extended all the way across NL.

A stronger indication of the early positional specificity of the dorsal terminal fields was shown in five chicks in which more than one NM neuron was filled at E9–E10. Figure 6 shows planar projections from two of these animals in each of which two NM cell bodies close to one another were filled with HRP. The accompanying planar projections of NL suggest that even when NM somata are within a few microns of each other, their ipsilateral terminal fields, though overlapping, are ordered in the same way—the more medial or posterior soma having the more medial or posterior terminal field, etc. This correspondence suggests that the early projections of NM onto the ipsilateral NL already exhibit a very high degree of positional specificity. Since the ventral terminal fields were separated from their contralateral cell bodies by the injection procedure they could not be studied in this way.

Quantification of the terminal field planar projections was carried out as detailed above (Materials and Methods). Area and width were measured for all terminal fields. Length was measured for dorsal terminal fields to derive the parameters L/W, a measure of terminal field elongation. Ventral terminal fields were fully extended across NL at all ages. Angle was measured only in ventral terminal fields at E9, since at this age the dorsal terminal fields were not oriented. The length of NL along its tonotopic axis was measured and the ratio of terminal field width to the NL length, the width/nuclear-length ratio (W/Ln), was calculated. Table 2 summarizes these measures at E9. Significant differences occurred in W/Ln between dorsal ($\bar{X}$ = 0.19) and ventral ($\bar{X}$ = 0.24), and between anterior ($\bar{X}$ = 0.21) and posterior ($\bar{X}$ = 0.27) groups of terminal fields. The greater W/Ln between dorsal and ventral terminal fields is accompanied by a large and significant dorsal/ventral difference in area (A). The smaller area and W/Ln dorsally probably reflect the relative immaturity of dorsal terminal fields in size and shape (note that dorsal elongation is slight, L/W < 2).

Terminal morphology. At E9 both dorsal and ventral axons are sparsely branched within NL. Figure 7 is a photomicrograph of dorsal NM terminals at E9. The main axon branches are fine, mostly less than 0.5 μm in diameter. Short, very fine appendages ($\leqslant$ 20 μm long, about 0.2 μm diameter) are common at the tips and along the courses of the axons. Thin, veil-like structures are commonly found along the axons, at branch points, and especially at the terminals. These appear to be growing axon tips.

Embryonic day 11

Branching pattern. Between E9 and E14 the ipsilateral (dorsal) terminal arborization expands into an elongated band. The presence, at E9, of long axonal branches terminating in growth cones that have not yet reached NL (Figs. 3,4) suggests that this expansion occurs, at least in part, by way of new branches from the main ipsilateral axon trunk. Figure 8 is a coronal reconstruction of a dorsal and a ventral axonal arborization at E11. It illustrates the increased number of branches in dorsal NL, as well as the tendency of the dorsal arborizations to elongate by adding new patches of terminals. Indeed, the arborization of TF 48 (E11, Figs. 8, 10A) is very similar to that of TF 18 (E9, Figs. 3, 5b) with the addition of a lateral patch of terminals. We should emphasize that we have never observed a dorsal axon branch traversing across many cells within NL and arborizing in several separate patches (as often happens on the ventral side, e.g., TF 49, Fig. 8). Thus, it is unlikely that elongation of the dorsal terminal fields results from axon growth within NL, where it might receive guidance

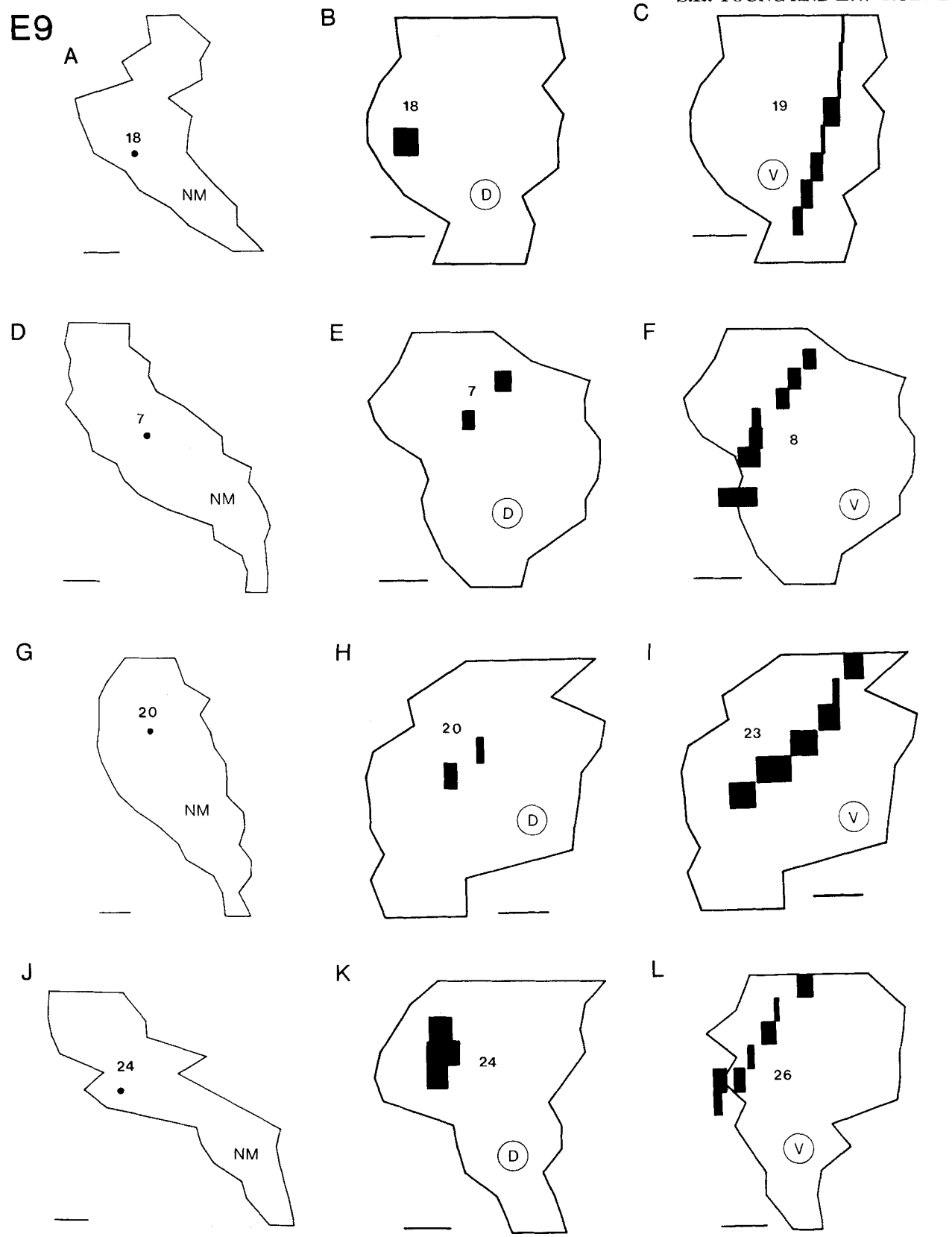

Fig. 5. Planar projections from E9 embryo showing the positions of cell bodies in NM (left column), their respective dorsal terminal fields in NL (middle column), and ventral terminal fields in the same nuclei (C,F,I) or in the same brain in the contralateral NL (L). All nuclei are drawn as if on the right side; anterior is up, midline is to left. Cells and terminal fields are labelled with TF numbers. Dorsal terminal fields are indicated by circled D, ventral terminal fields by circled V. NM somata and terminal fields are similarly located in their respective nuclei. Ventral terminal fields are fully extended across NL. Bars = 0.1. mm.

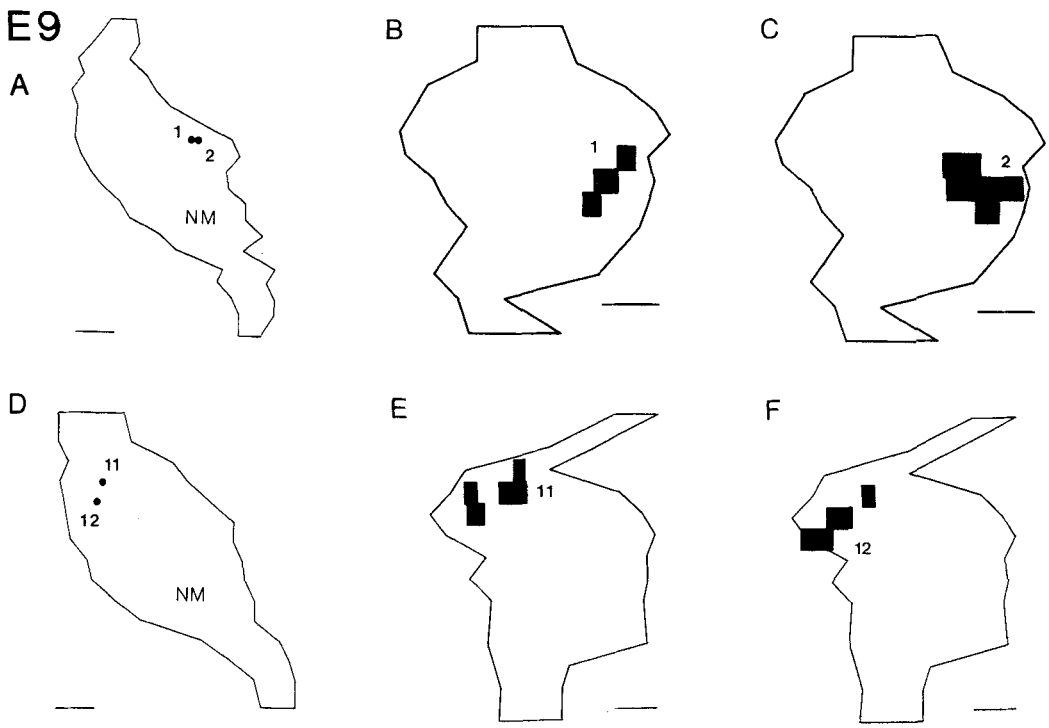

Fig. 6. Planar projections of NM and NL at E9. Cell bodies and terminal fields are identified by the adjacent numbers. A and D show cell body locations in NM. B, C, E, and F show terminal fields whose positions suggest a spatial order similar to that of their cell bodies. Bars = 0.1 mm.

from its target cells. Instead, we believe that the new collaterals develop from the parent axon remote from its endings in NL. The new collaterals are then somehow guided to appropriate positions within what will become appropriate positions within an isofrequency band.

Figure 8 also illustrates the increased length and complexity of the terminal branches from the contralateral NM that arborize on the ventral side of NL at E11.

Terminal fields. Despite the observation that elongation of the dorsal terminal fields between E9 and E14 is mediated by axons branching off the main trunk at points well outside of NL, the orientation of the elongating terminal fields is not random. In Figure 8 the more lateral patch of dorsal terminals is well anterior of the medial patch. The initial elongation is already roughly perpendicular to what will be the NL tonotopic axis. This is best observed in planar projections of the terminal fields (Figs. 9, 10). Even though the dorsal terminal fields in these figures are not fully elongated, they can be seen to extend along roughly the same orientation as the ventral terminal fields in the same nuclei.

E11 terminal field planar projections were quantified in the same way as those at E9, with an additional parameter on the dorsal side, angle, that measures the orientation of the terminal fields (Table 3). The angle measurements clearly show that, although the variability of dorsal terminal field angle is high, the mean angle on the dorsal and ventral sides is essentially the same. Ventral terminal fields at E11 continue to be significantly larger in area than dorsal terminal fields.

Terminal morphology. The morphology of the terminal arborizations between E10 and E13 appears transitional. On many axons velate growing tips are still common, though these are more highly arborized than at E9 (Fig. 11A). Other axons have lost the veillike structures and are even more highly arborized (Fig. 11B). These axons are marked by the abundant profusion of extremely fine, sinuous branches of filopodia and spikes similar to immature endings described in other systems (e.g., Morest, '68; Mason, '82). The major branches of the axon trunks increase in diameter during this period, ranging up to about 1 μm.

Embryonic days 14–17

Branching pattern. At E14 the mature pattern of the terminal arborizations is achieved in both dorsal and ventral NL neuropil. We have described previously a banded pattern of terminals qualitatively similar to the pattern described below in late embryos and chickens up to 1-month posthatch (Young and Rubel, '83). In the present study 11 reconstructed terminal fields from one stage 43 (E17) embryo are included to confirm this similarity. Figures 12 and 13 illustrate the mature NM axon arborization pattern. The primary bifurcation of the axon ventral and medial to the NM cell body leads to arborizations in NL on both sides of the brain. The contralateral terminals derive from a succession of branches projecting into NL from the main axonal trunk as it courses anterolaterally across the convex ventral face of NL. The ipsilateral axon branch loops back through or above NM toward the ventricular surface and then turns ventrally to where it radiates branches into the concave dorsal NL neuropil. Figures 12 and 13 also illustrate the full extension of the dorsal terminal fields across the width of NL. Extension of the dorsal terminal fields has been accompanied by an increase in their patchiness.

On the ventral side, the earlier sparse arborization of the axon throughout its course below NL has been replaced by

TABLE 2. E9 Terminal Field Measurements[1]

		Area (A) (μm^2)		Width (W) (μm)		L/W		W/Ln		Angle (degrees)	
Dorsal mean	(n)	5,550	(8)	93	(8)	1.84	(8)	0.19	(8)	–	
	(SE)		(1,149)		(14)		(.28)		(.03)		
Ventral mean	(n)	10,450	(18)	120	(18)	–		0.24	(18)	92.3	(18)
	(SE)		(1,213)		(8)				(.01)		(2.3)
Anterior mean	(n)	8,300	(19)	105	(19)	1.88	(6)	0.21	(19)	93.1	(13)
	(SE)		(1,072)		(8)		(.29)		(.01)		(2.9)
Posterior mean	(n)	10,700	(7)	129	(7)	1.74	(2)	0.27	(7)	90.4	(5)
	(SE)		(2,352)		(16)		(.99)		(.03)		(3.4)

[1]Area (A), width (W), length/width ratio (L/W), width/nuclear length ratio (W/Ln), and angle measurements (see Fig. 2) shown for terminal fields grouped by side (dorsal or ventral) or position (anterior or posterior). Mean, standard error of the mean (SE), and number of observations (n) shown for each group.

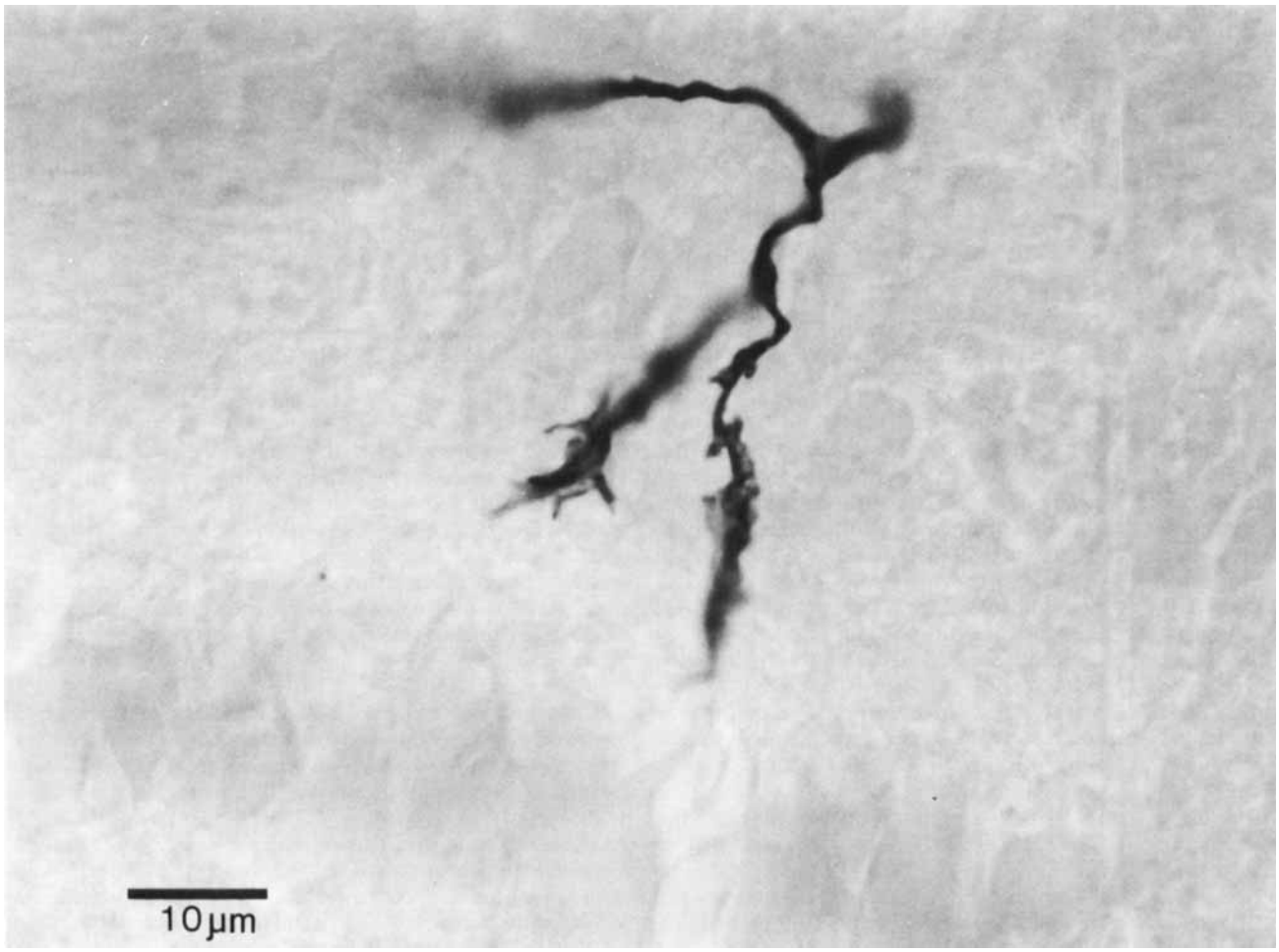

Fig. 7. HRP-stained NM axon terminals in dorsal NL neuropil at E9. The unstained cell bodies below the terminals are NL neurons. The lightly textured area through which the terminal growth cones pass is the dorsal NL neuropil. These are the medial branches of TF 7, also shown in Figures 4 and 5E. Bar = 10 μm.

a highly arborized termination, also distributed in patches across NL.

Terminal fields. At E14–17 both the dorsal and ventral terminal fields are narrow bands across NL, usually composed of two or three irregular patches of terminals. Often these patches can be seen in the terminal field planar projections (Figs. 14, 15). These figures also show the full extension of the dorsal terminal fields. Dorsal and ventral terminal fields have become comparable in shape and orientation.

Measurements of the E14–17 terminal fields are summarized in Table 4. Both dorsal and ventral terminal fields have increased in absolute area and are no longer significantly different. Total width is significantly greater than at E11. Nevertheless, L/W is significantly greater and W/Ln is significantly less than at E11. As at E9, a significant

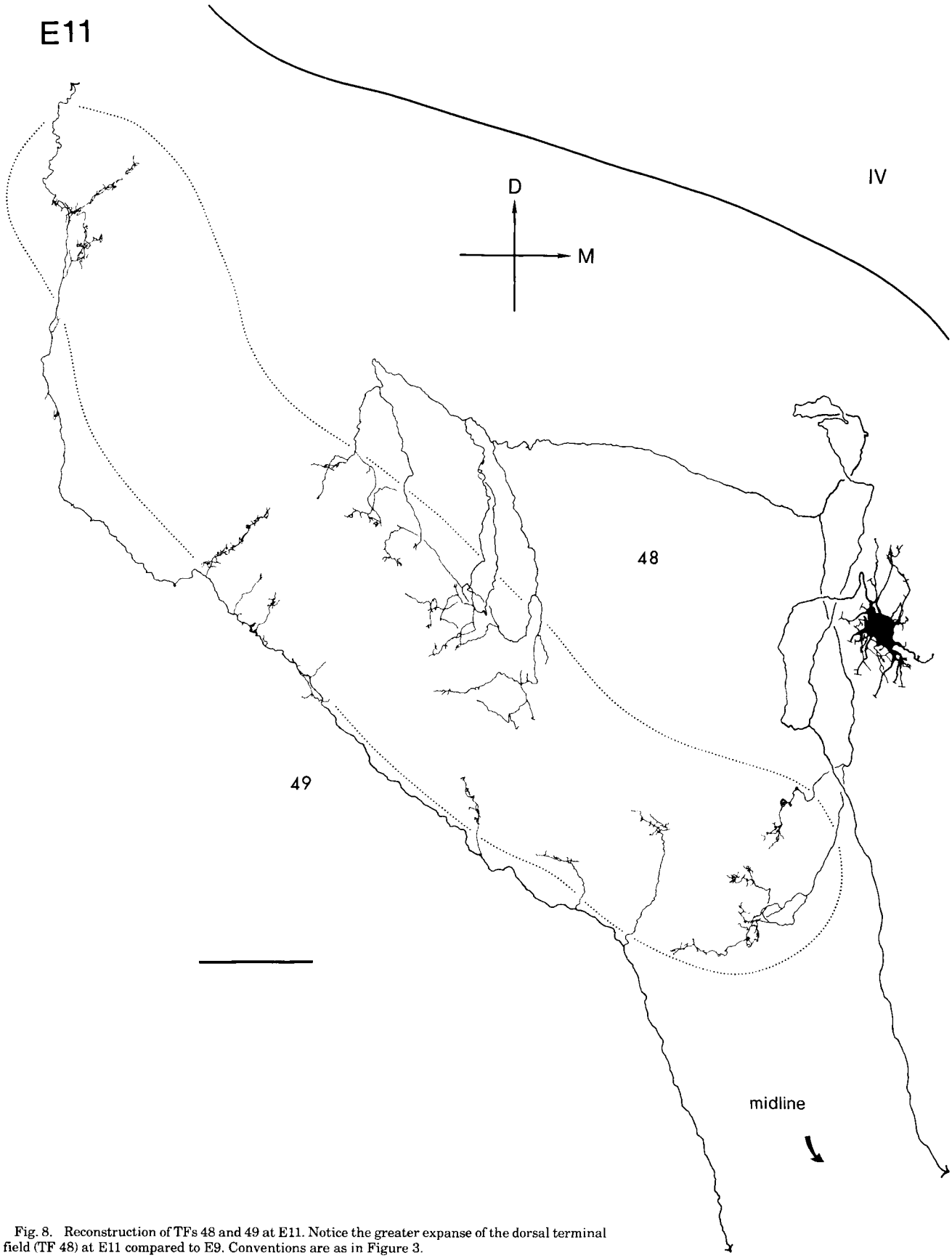

Fig. 8. Reconstruction of TFs 48 and 49 at E11. Notice the greater expanse of the dorsal terminal field (TF 48) at E11 compared to E9. Conventions are as in Figure 3.

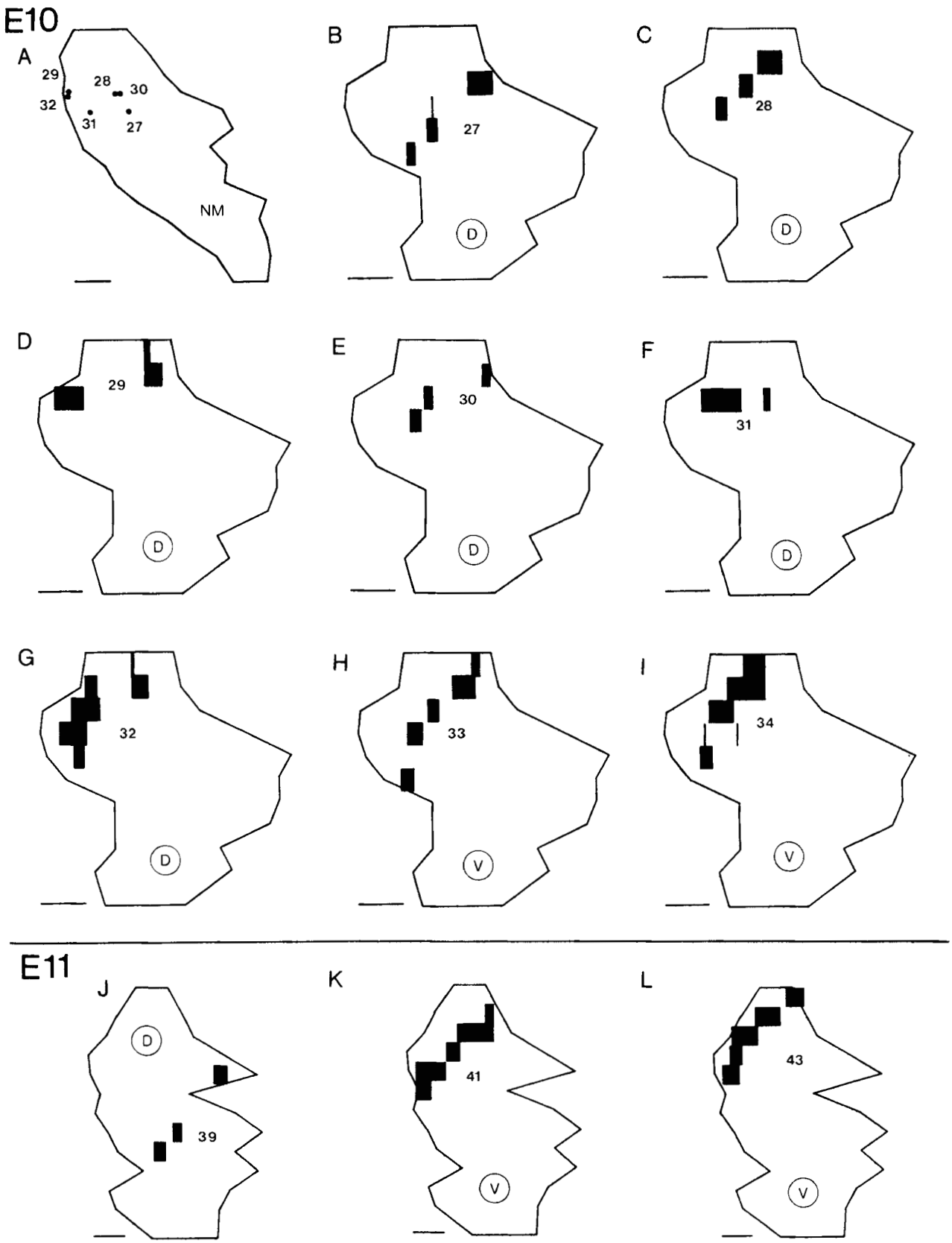

Fig. 9. Planar projections showing dorsal and ventral terminal fields in NL and six cell bodies in NM (A). Dorsal terminal fields indicated by circled D, ventral terminal fields by circled V. A–F are all from the same side of one 10-day embryo. G–I are from one E11 chick. Dorsal terminal fields are more elongated than at E9 and extend generally in orientations similar to those of their ventral counterparts. Midline is to left, anterior up. Bars = 0.1 mm.

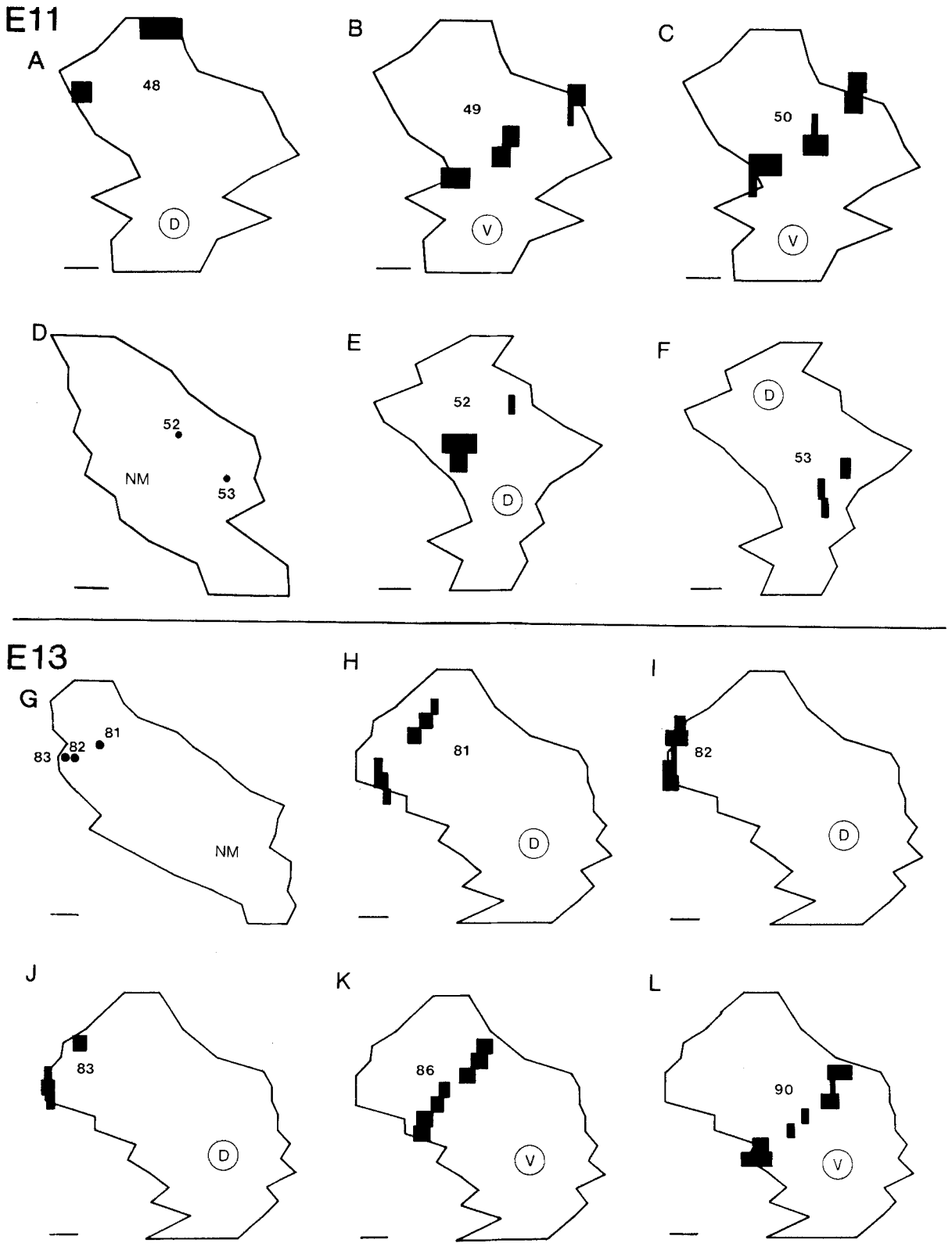

Fig. 10. Planar projections showing E11 (A–F) and E13 (G–L) cell bodies and terminal fields. A–C are from one NL, D–F from another brain, and G–L from a third. Dorsal terminal fields are less elongated and less consistently oriented than ventral terminal fields at this age. Conventions are as in Figure 9. Bars = 0.1 mm.

TABLE 3. E11 Terminal Field Measurements[1]

		Area (A) (μm^2)	Width (W) (μm)	L/W	W/Ln	Angle (degrees)
Dorsal mean	(n)	8,950 (19)	141 (19)	2.12 (19)	0.21 (19)	93.3 (19)
	(SE)	(1,050)	(11)	(.22)	(.02)	(5.2)
Ventral mean	(n)	14,925 (23)	138 (23)	–	0.19 (23)	92.1 (22)
	(SE)	(1,189)	(6)		(.01)	(1.6)
Anterior mean	(n)	11,525 (33)	139 (33)	1.99 (16)	0.20 (33)	93.5 (32)
	(SE)	(1,014)	(7)	(.21)	(.01)	(3.2)
Posterior mean	(n)	14,775 (9)	141 (9)	2.83 (3)	0.19 (9)	89.9 (9)
	(SE)	(2,075)	(10)	(.83)	(.01)	(2.4)

[1]Area (A), width (W), length/width ratio (L/W), width/nuclear length ratio (W/Ln), and angle measurements (see Fig. 2) shown for terminal fields grouped by side (dorsal or ventral) or position (anterior or posterior). Mean, standard error of the mean (SE), and number of observations (n) shown for each group.

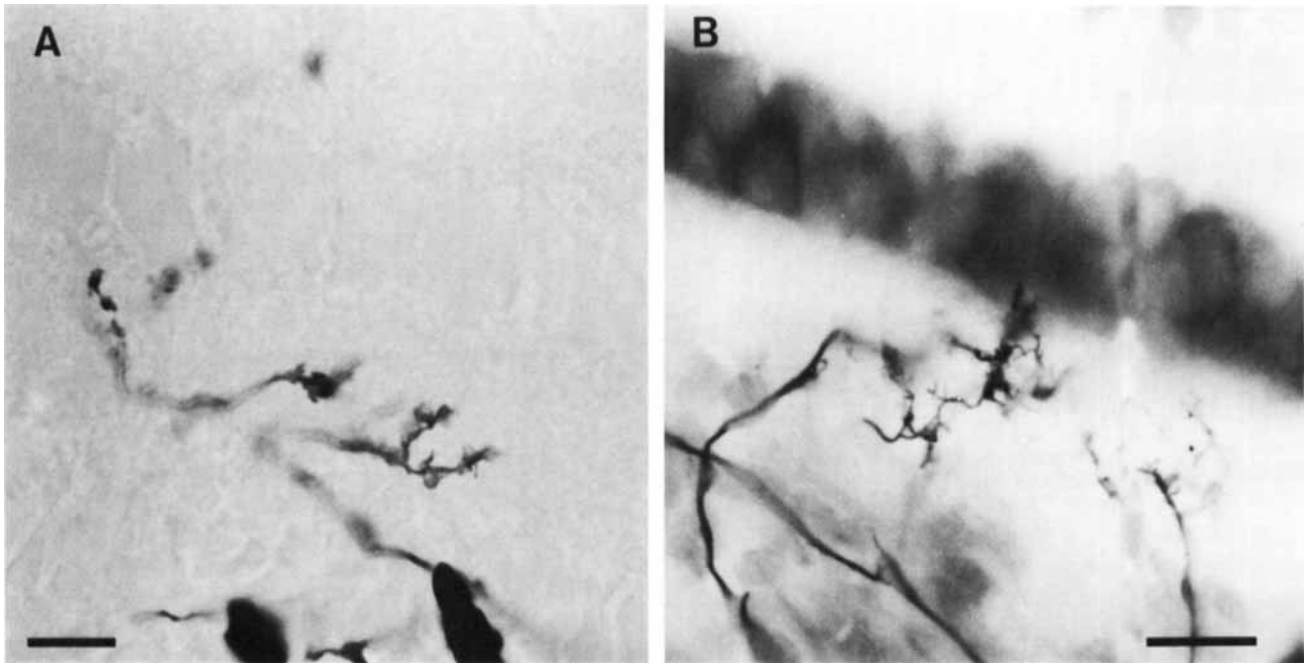

Fig. 11. A. Veiled growing tips of NM axons in ventral neuropil of E11 NL. Unstained blocky shapes above the terminals are NL cells. The more finely textured area below is ventral NL neuropil. A segment of the axon from which this arborization comes can be seen between the two dark masses at lower center. The dark masses are red blood cells. B. Profuse, very fine terminal branches in ventral NL neuropil at E11. NL is the dark layer of cells from upper left to center right with clear neuropil layers above and below. Counterstained with toluidine blue. Bars = 10 μm.

anterior/posterior difference in W/Ln is seen. There is no difference between dorsal and ventral W/Ln. The variability of dorsal AN is reduced and is now comparable to that of the ventral terminal fields. Thus, the dorsal terminal fields have lengthened, narrowed, and tightened their orientations so that by E14 they lie directly in register with the ventral terminal arborizations.

Terminal morphology. At E14–E17 velate growing tips are no longer seen. Many axons at E14 still have the profuse, fine arborizations that appeared at E11, though the preterminal branches have thickened somewhat. Other E14 axons have lost these fine processes and have begun to develop clusters of small boutons (Fig. 16). By E17 the thickening of preterminal branches has progressed further. Terminal arborizations are noticeably less dense and termination in clusters of boutons has become the rule (Fig. 17). No changes in the morphology of the endings have been observed subsequent to E17.

The development of registry between dorsal and ventral terminal arborizations

Dorsal and ventral terminal fields have very different patterns at E9, about when NM axons first appear in the dorsal NL neuropil (see following section). The ventral terminal fields are elongated and uniformly oriented across NL. The dorsal terminal fields, on the other hand, tend to be punctate and are already in appropriate positions with respect to their cell bodies' locations in NM. In this section we summarize the quantitative and qualitative changes that appear to bring the ipsilateral and contralateral inputs to NL into registry.

Ventral terminal field shifts. For the sake of simplicity, we have only indicated the areas of terminal arborizations within the NL neuropil in the terminal field planar projections shown above. The course of the axon was not shown. However, an important observation can be made when the

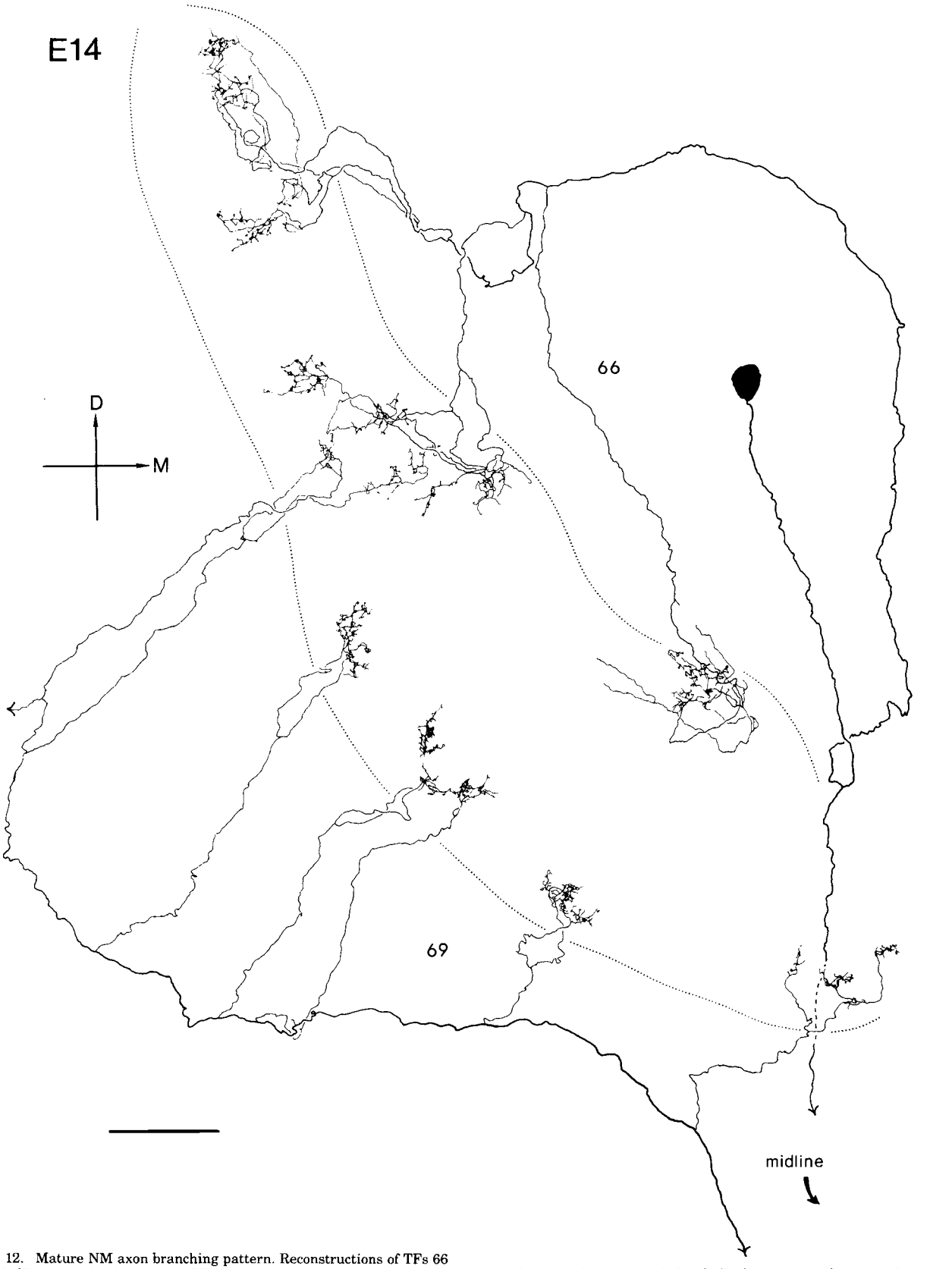

Fig. 12. Mature NM axon branching pattern. Reconstructions of TFs 66 and 69. The ventral arborization (TF 69) is shown shifted to the right to save space. The width of the medial end of NL (dotted line) is thus exaggerated. Note the difference in dorsal and ventral branching patterns—dorsal terminal patches being extended radially from a central point and ventral branching points occurring in regular succession along the ventral axon. Conventions as in Figure 3. Bar = 10 μm.

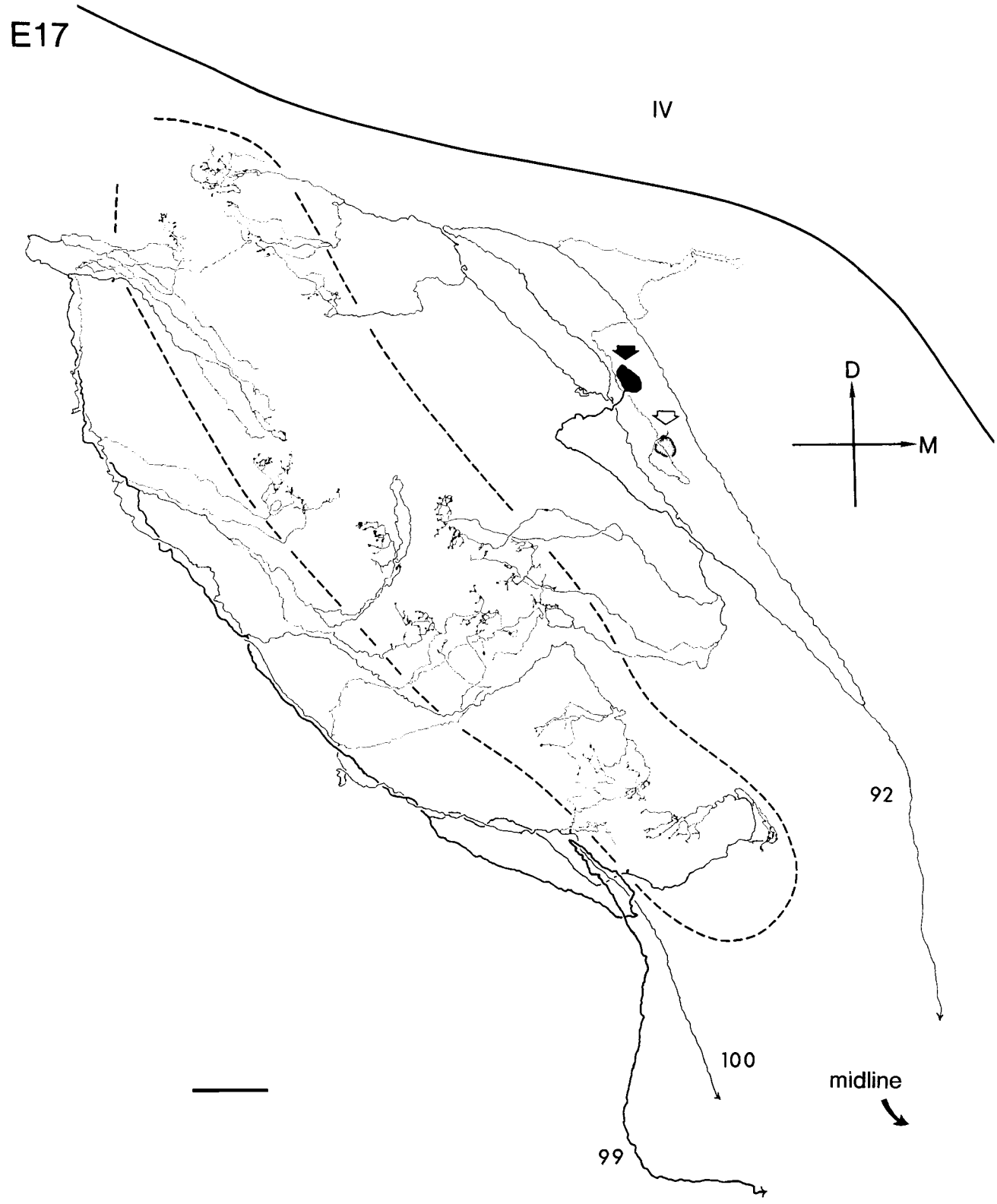

Fig. 13. Reconstructions of one dorsal (TF 92) and two ventral (TFs 99, 100) NM axon arborizations at E17. The scale of this drawing is reduced from previous reconstructions. The two ventral axons are twined around one another, yet the terminals of the thicker axon (TF 99) are consistently shifted to the right of those of TF 100 (see text). The cell body of the dorsal arborization (TF 92) is marked by the filled arrowhead. Its ipsilateral axon has a very fine branch that courses several hundred microns posteriorly beneath the ventricular floor and then dips down into NM and ends in a boutonlike structure apposed to another NM neuron (open arrowhead). This bouton is shown in Figure 30B. Conventions as in Figure 3. Bar = 10 μm.

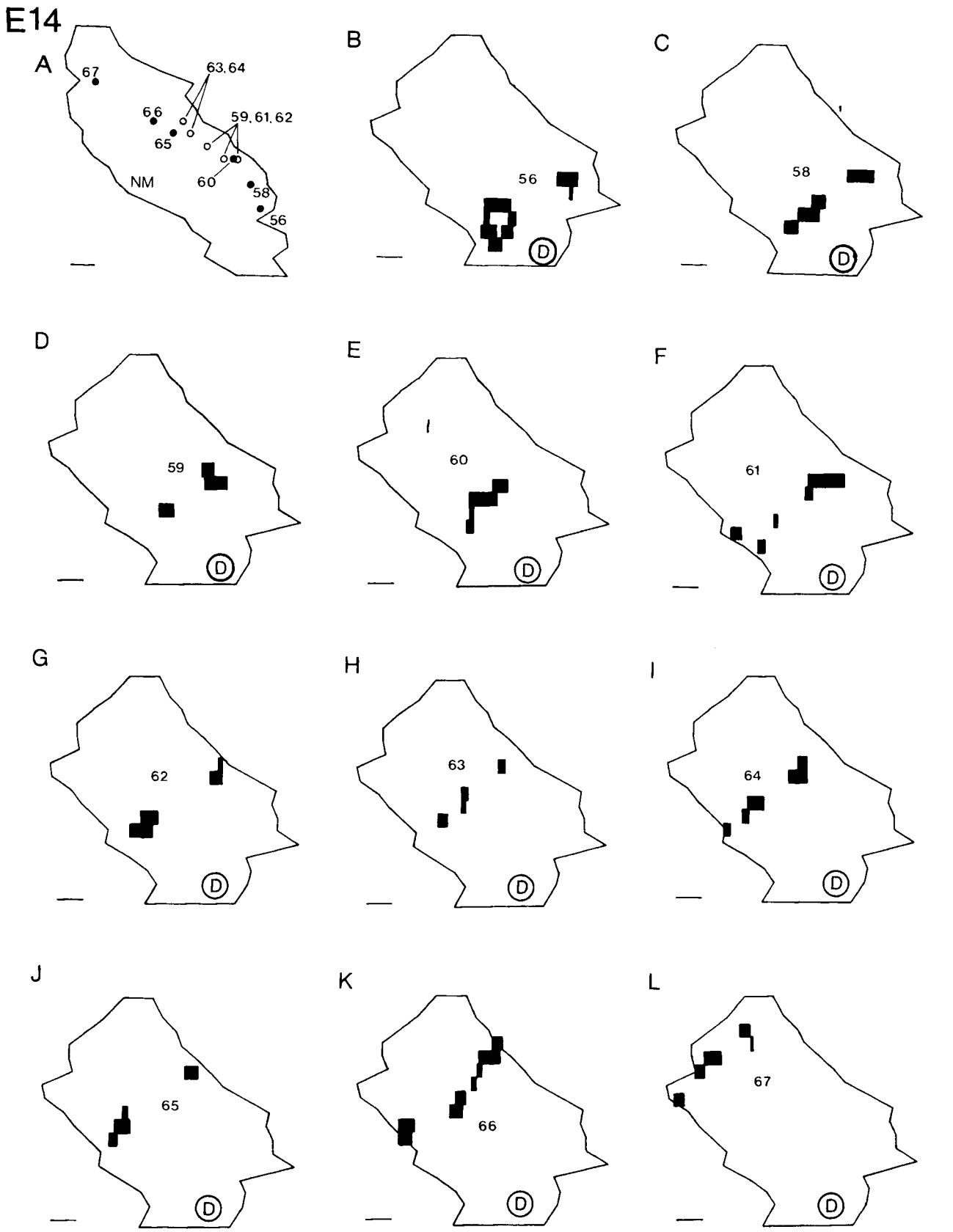

Fig. 14. Planar projections showing terminal fields at E14. B–L are dorsal terminal fields in the same NL. Their cell body positions are shown in A. Two sets of cells (63 and 64; and 59, 61, 62) whose connections with their terminal fields could not be clearly distinguished are shown by open circles. The cell bodies marked by solid circles were positively identified with their respectively numbered terminal fields. Anterior is up; midline is to left. Bars = 0.1 mm.

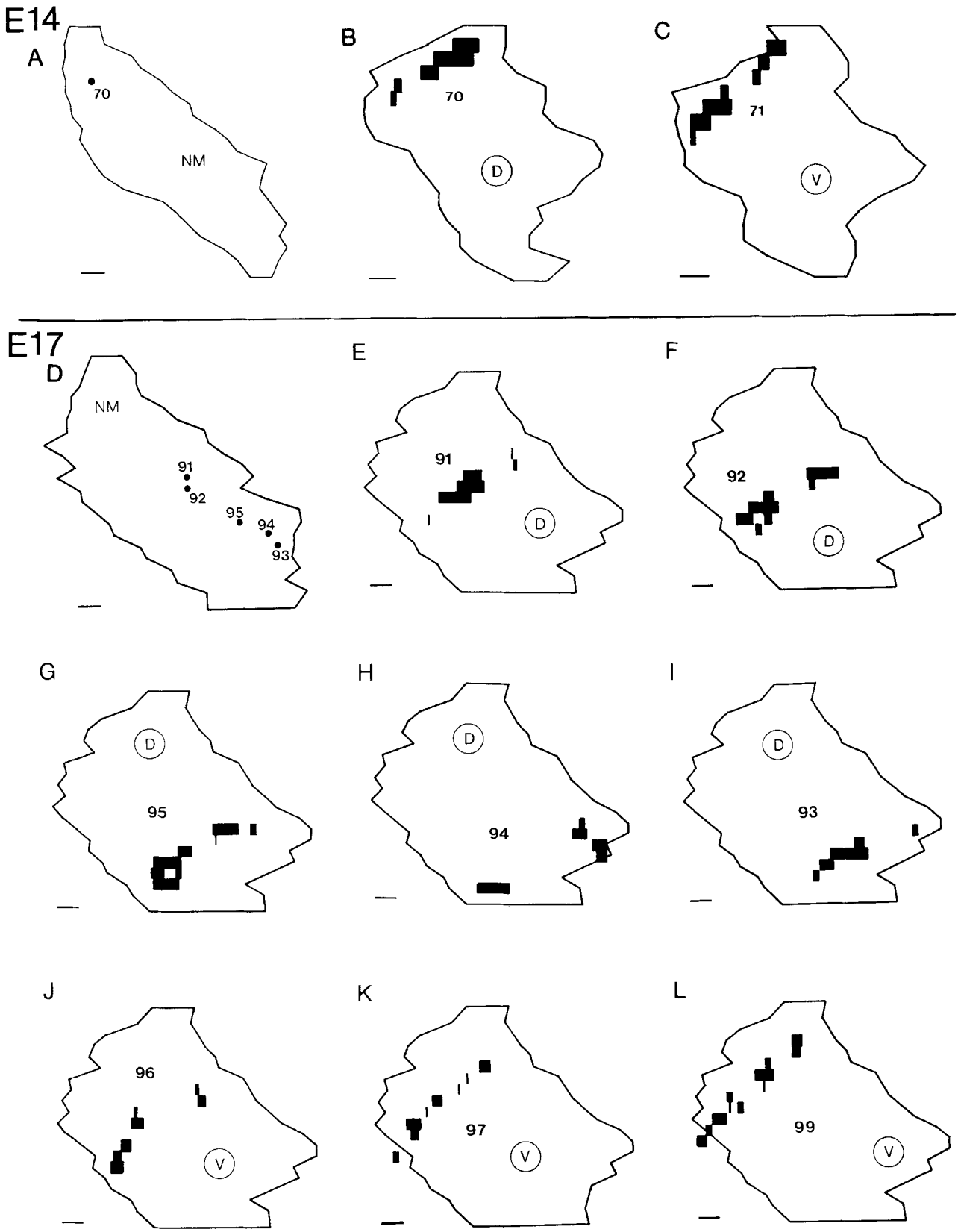

Fig. 15. Planar projections showing dorsal and ventral terminal fields in NL and cell body positions in NM. Dorsal terminal fields indicated by circled D, ventral terminal fields by circled V. A–C are from one chick at E14. D–L are from an E17 brain. Dorsal and ventral terminal fields are both fully extended and uniformly oriented across NL. The continuing correspondence between the order of positions of cell bodies and their dorsal terminal fields suggests that, in contrast to ventral terminal fields (see text), the dorsal terminal fields do not shift appreciably between E9 and E17. Anterior is up, midline to left. Bar = 0.1 mm.

TABLE 4. E14 Terminal Field Measurements[1]

		Area (A) (μm^2)	Width (W) (μm)	L/W	W/Ln	Angle (degrees)
Dorsal mean	(n)	14,850 (20)	156 (20)	2.87 (20)	0.16 (20)	85.3 (19)
	(SE)	(1,291)	(10)	(.18)	(.01)	(1.6)
Ventral mean	(n)	17,150 (13)	165 (13)	—	0.16 (13)	91.3 (12)
	(SE)	(1,782)	(10)		(.01)	(2.3)
Anterior mean	(n)	15,200 (20)	148 (20)	3.33 (11)	0.15 (20)	89.1 (20)
	(SE)	(1,174)	(8)	(.19)	(.01)	(1.6)
Posterior mean	(n)	16,600 (13)	176 (13)	2.32 (9)	0.18 (13)	84.8 (11)
	(SE)	(2,011)	(12)	(.23)	(.01)	(2.5)

[1]Area (A), width (W), length/width ratio (L/W), width/nuclear length ratio (W/Ln), and angle measurements (see Fig. 2) shown for terminal fields grouped by side (dorsal or ventral), or position (anterior or posterior). Mean, standard error of the mean (SE), and number of observations (n) shown for each group.

relationship between the ventral terminal arborizations and the courses of their main axons is examined. Figure 18 shows 11 examples of planar projections of ventral terminal fields at E9–E15 with the axon paths indicated by dashed lines. These examples illustrate that ventral terminal arborizations before E14 (Fig. 18A–F) are invariably closely associated with their parent axon trunks. By E14 and thereafter, however, the positions of ventral terminal arborizations often differ markedly from the positions of their axons, either anteriorly or posteriorly (Fig. 18G–I).

Additional evidence suggests that the separation of ventral axons and their terminal fields at E14 represents movements of the terminal fields along the NL tonotopic axis. Figure 19 shows two pairs of ventral terminal fields and their respective axons from the same E17 chick. Both pairs of axons are closely fasciculated, the axons looping around one another as they course beneath NL (see Fig. 13). At E9–E13 all ventral terminal fields closely overlie their axons. Since these intertwined axons could not have moved with respect to one another, the terminal fields shown in Figure 19 must originally have overlain each other. Yet, by E17 these terminal fields have shifted away from their axons by different amounts and even in different directions. This suggests that when the early ventral axons grow into NL from the contralateral NM, they do not have the same topographic precision as their ipsilateral counterparts, and that the mature ventral topographic order is not established until E14 or later (see Discussion).

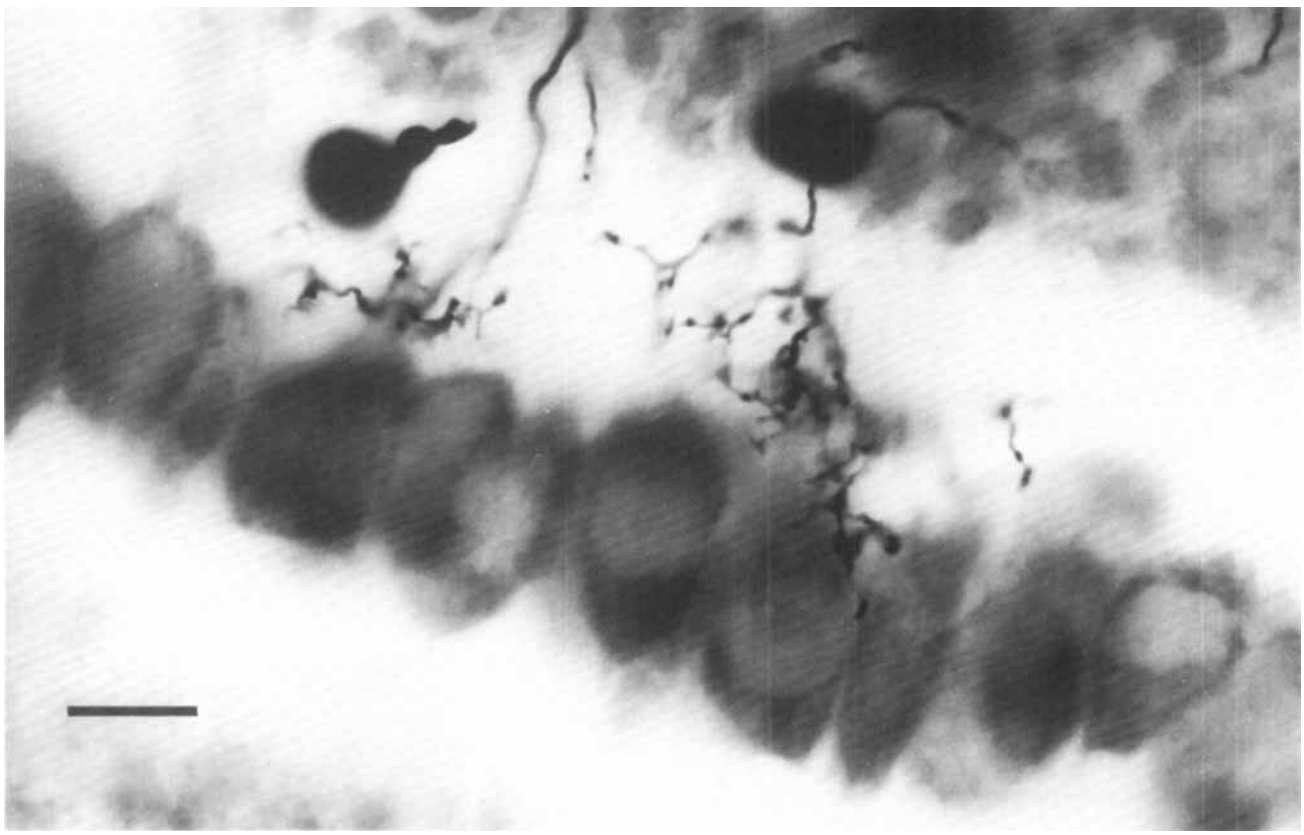

Fig. 16. Photomicrograph of NM terminals in dorsal NL neuropil at E14. The line of somata with clear areas above and below is NL. Small boutons appear along and at the ends of the terminal axon branches. The round black masses are red blood cells. Section was counterstained with toluidine blue. Bar = 10 μm.

Fig. 17. Dorsal NM terminals at E17. Terminal boutons and *en passant* swellings are more prominent than at E14. The round black masses are red blood cells. Counterstained with toluidine blue. Bar = 10 μm.

Dorsal terminal field elongation. Figure 20 shows the major changes we have observed in dorsal terminal arborizations between E9 and E17. On the left, planar projections of three representative terminal fields are shown. To the right of each planar projection is a schematic, three-dimensional rendition of the axon trajectory and terminal field shape at each age. It is important to realize that the elongation and alignment of arbors constitute a gradual process, not a series of discrete stages, as must be depicted diagrammatically.

At E9 the ipsilateral axon has made its circuitous path, first ventrad to bifurcate, then returning dorsally through NM, only to course slightly rostral and then ventral again to end in the dorsal neuropil of the ipsilateral NL. The simple elongated growth cones terminate in a restricted region of NL, often a single spot. This projection appears to precisely be topographic; the positions of terminals match the position of the parent cell body in NL, and adjacent NM cell bodies have overlapping terminal fields that are slightly displaced from one another in the same direction as their parent cell bodies. Between E9 and E11 the terminal fields begin to elongate in the caudomedial to rostralateral dimension that matches the orientation of ventral axons and terminal arbors. Surprisingly, the elongation does not arise from branches within NL but from entirely new collaterals from the parent axon. At E11–E12 the arbors tend to terminate in a complex proliferation of delicate processes, and they are often slightly misaligned, as shown in Figure 20B. By E14 the delicate terminal processes are becoming pruned into definitive boutons and the separate arbors have become aligned into a distinctive elongated band whose orientation precisely matches that of the ventral terminal arbors. Throughout this period the dorsal terminal fields appear to maintain a precise topographic map of the position of their NM somata along the tonotopic axis, as evidenced by the fact that when multiple cells were reconstructed the order of NM cell bodies along this axis was always preserved in the order of terminal fields. While we cannot contend that the elongated terminal fields do not shift their position within NL, if they do so it must take place in an orderly manner such that adjacent axons all shift in the same direction and approximately the same distance, which is distinctly different from their ventral counterparts.

Quantitative comparisons. Statistical comparisons of terminal field parameters presented in Tables 2–4 confirm the observations diagramed above. The major developmental trends are summarized in Figure 21. Terminal field area (Fig. 21A) increases steadily from E9 to E14 and probably continues to increase, at least through E17. Dorsal terminal fields were initially smaller than ventral terminal fields but by E14 this difference failed to reach statistical significance and by E17 they were of identical size. Analysis of Area (A) measurements showed significant main effects of age (F (2, 89) = 14.4, $P < .001$), and side, dorsal, or ventral (F (1, 89) = 16.53, $P < .001$). However, the interaction failed to reach statistical significance (F (2, 89) = 1.0, $P = .37$).

Terminal fields also grow slightly in absolute width, probably at least until E17 (Fig. 21B). Posterior terminal fields (low-frequency region of NL) are slightly but consistently wider than anterior terminal fields. There were no reliable differences between dorsal and ventral terminal field widths. An ANOVA revealed main effects for age (F (2, 89) = 10.85, $P < .001$) and position, anterior or posterior (F (1, 89) = 4.39, $P = .039$). The interaction did not approach statistical significance.

The L/W measurements provide an estimate of the elongation of the terminal fields. Since the ventral terminal fields were fully elongated at all ages this parameter was only calculated for the dorsal terminal fields. The increase in elongation of the dorsal terminal fields over age is illustrated in Figure 21C. It is evident that the increase in absolute width (Fig. 21B) is more than compensated for by a disproportionate growth of the dorsal terminal fields in length across NL. The data at E17 suggest that dorsal terminal fields are fully elongated by E14. An ANOVA revealed a main effect of age (F (2, 41) = 7.32, $P = .002$), and an interaction between age and position, anterior or posterior (F (2, 41) = 4.5, $P = .017$). The interaction of age and position (not shown) indicates that posterior terminal fields elongate earlier than anterior terminal fields. This is puzzling in light of the rostrocaudal gradient of development usually seen in NM and NL (Rubel et al., '76; Parks and Jackson, '84).

The proportion of the NL frequency axis covered by the terminal field is described by W/Ln Fig. 21D). The smaller this number, the greater the "frequency specificity" of the axonal arbors. This parameter of the ventral terminal fields decreases from almost 25% to about 16% between E9 and E14. On the dorsal side W/Ln also decreases between E11 and E14 from 21% to 16%. Frequency specificity of terminal arbors appears to remain constant after E14. Like width, W/Ln was greater posteriorly. The ANOVA revealed significant main effects of age (F (2, 89) = 13.27 , $P < .001$) and

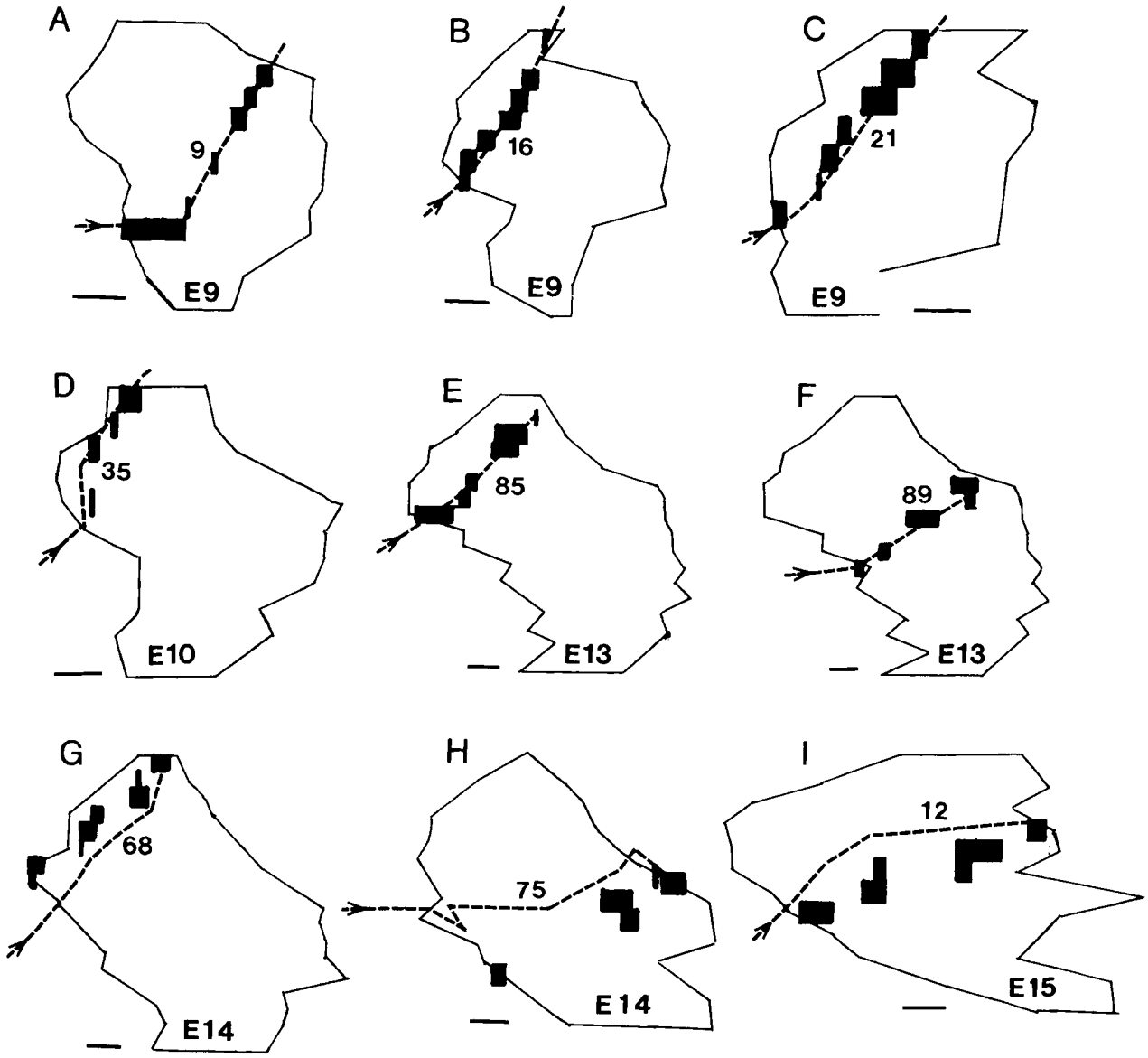

Fig. 18. Planar projections showing the relationship of ventral NM axons to their terminal fields in NL between E9 and E15. The ages of the animals are indicated on each planar projection. The paths of the ventral axon trunks are shown by the heavy dashed lines. In planar projections of NL at ages less than E14 ventral terminal fields are always closely associated with the ventral axon trunk. At E14 and beyond the terminal arbors tend to be shifted either rostral or caudal of their main axon trunk. Anterior is up, midline to left. Bars = 0.1 mm.

position, anterior or posterior (F (1, 89) = 4.86, P = .03). Figure 21D illustrates the overall decrease in W/Ln over age and also an interesting interaction between age and side (dorsal or ventral, F (2, 89) = 3.37, P = .039). Frequency specificity of dorsal terminal fields is initially much greater (lower W/Ln) and more variable than that of ventral terminal fields. By E11 ventral W/Ln has decreased and dorsal W/Ln is less variable, and by E14 dorsal and ventral W/Ln are essentially the same. An age by position interaction was also seen in W/Ln (F (2, 89) = 3.6, P = .031, not shown). The posterior terminal fields acquired their mature frequency specificity sooner than did the anterior terminal arbors.

The angle (AN) of all terminal fields was also measured, except on the dorsal side of NL at E9. Mean AN measurements were similar throughout the nucleus and at all ages (Tables 2–4).

Initial formation of the pathways

Several embryos at ages between E6 and E8 were injected with HRP in order to examine the genesis of the initially different patterns of dorsal and ventral terminal fields. Planar projections were not constructed at these early ages because of the small terminal arborizations and the indistinct boundaries of NM and NL. The following description of early pathway formation is based on successful experiments on two embryos at stage 29 (E6), two embryos at stage 31, one embryo at stage 32, and three embryos at stage 34 (E8).

NM axons first reach the ipsilateral NL on E8 (Fig. 22). Their terminals resemble those described at E9. Surprisingly, the contralateral axon branches reach their targets prior to E8. A few HRP-filled NM axons have been found wandering unbranched through the contralateral ventral NL as early as E6. This fact allowed us to fill very young

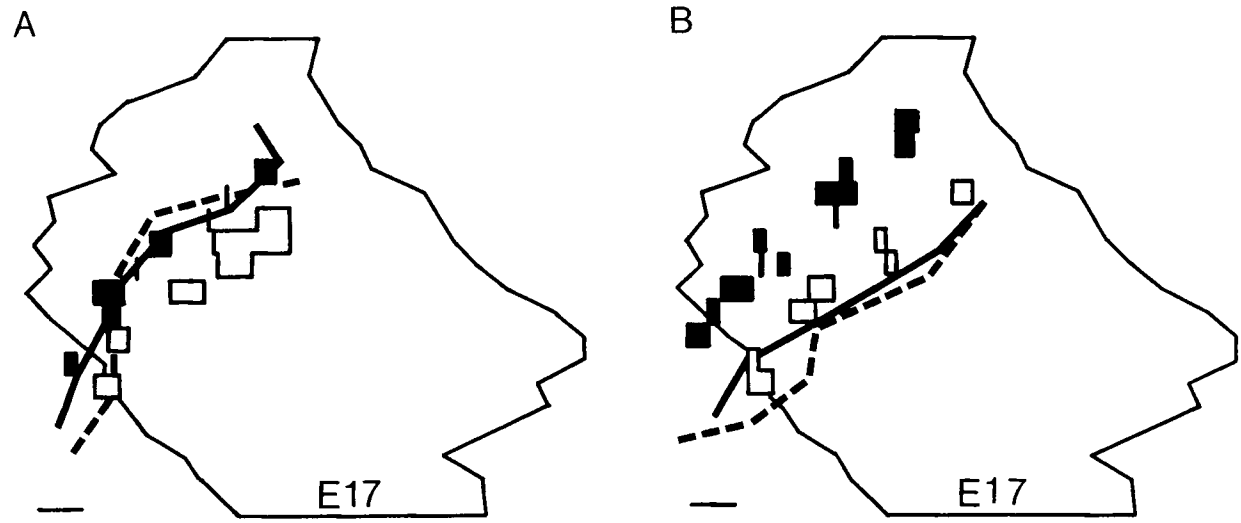

Fig. 19. Planar projections showing two pairs of NM axons and terminal fields in one E17 NL. A shows TF 97, solid line and rectangles, and TF 98, dashed line and open rectangles. B shows TF 99, solid line and rectangles, and TF 100, dashed line and open rectangles. TF 98 is shifted posterolaterally from its axon. TF 99 and TF 100 are both shifted anteromedially from their axons but by widely different amounts. TF 99 is now distant from its axon by about 25% of the total NL length. Anterior is up, medial to left. Bars = 0.1 mm.

NM axons with the same techniques used at later stages and to study the early growth of the ipsilateral axon branch.

Figure 23B shows an HRP-filled NM neuron in the dorsolateral quadrant of the medulla at E6. Its contralateral axon branch, which courses beneath the more darkly stained ventricular zone, was backfilled with HRP from an injection at the midline (lower left of the figure). Figure 23A is a camera lucida drawing of the same NM neuron. Its axon courses ventromedially from the cell body (or a proximal dendrite) to a complex bifurcation 35 μm away. The ipsilateral branch is seen to reflect dorsolaterally and terminate in a growth cone, 40 μm from the soma, among the cells of the ventricular zone.

A similar NM neuron from the opposite side of the same brain is shown in a camera lucida drawing in Figure 24A. Its terminal growth cone has also grown in a direction away from its eventual target site in NL to course dorsolaterally into the ventricular proliferation zone (Fig. 24B). The two additional neurons successfully filled at E6 also showed the same pattern.

By E7 the ipsilateral NM axons have progressed further. The axons take a sharp turn away from the ventricular layer and extend straight toward the neurons in NL (Fig. 25). These axons, which end in a single growth cone above NL at E7, reach NL by E8 and begin to arborize (Fig. 22).

Contralateral NM axon branches course from their origins at primary bifurcations near their somata along the ventral border of the ventricular zone to the opposite side and, when earliest seen at E6, already wander through the coalescing group of NL neurons (Fig. 26). Their arborizations develop in complexity from unbranched at E6 to sparsely branched at E8 or E9. Very large HRP injections into the region of the crossed dorsal cochlear tract are required to backfill NM neurons at E6, suggesting that the few NM axons crossing the midline at that age are pioneer fibers (Harrison, '10).

Transient and infrequent projections

Four types of NM axonal projections occur that are not part of the general pattern described above. One of these is transient and may have developmental or phylogenetic implications that are not yet understood. Three others occur in relatively small numbers, but may be found to have secondary importance when the physiology of this system is better understood.

Anterior projection. A long, anterior projection of the contralateral axon branch is virtually universal in embryos up to 14 days of age (e.g., Fig. 26). Figure 27 shows a group of cells in the base of the cerebellum of a 9-day embryo, 600 μm rostral to the anterior pole of NL. This area appears to correspond to the processus lateralis cerebello-vestibularis (PCV), which is known to receive direct ipsilateral projections from ganglion cells innervating the macula lagena (Boord and Karten, '74). Three exceptionally well-stained contralateral NM axon branches reached this area by diverse routes and terminated in small arborizations. The absence of a well-defined tract is characteristic. Although many of these axons are stained for several hundred microns rostral to NL and can be traced well into the cerebellar peduncle, usually the HRP reaction product fades out before a terminal cluster is reached. Therefore, it is not known whether the region shown in Figure 27 is a common target of all the early contralateral axons.

The developmental changes in this projection are as follows. At E6 to E8, the earliest stages at which NM axons have been stained, the contralateral branch courses just under the ventricle to the posteromedial edge of the region where NL is beginning to coalesce (Fig. 26). The axon then makes a marked change in direction and begins to course predominantly rostrally, ventral to the incipient NL. When it reaches the anterolateral edge of NL it continues anteriorly without being in any way distinct from the portion lying beneath NL. Between E8 and E14 the axon passing under NL becomes dominated by its arborization in NL. This segment of the main axon grows severalfold in diameter. The anterior axon branch extending beyond NL does not grow and thus becomes marked by its smaller diameter. At this age the anterior branch leaves the NL arborization by turning sharply ventrad, away from the last of the axon's branches into NL (Figs. 4, 12, 28). By E17 the anterior branch is barely visible or absent. It has not been observed in posthatch chicks.

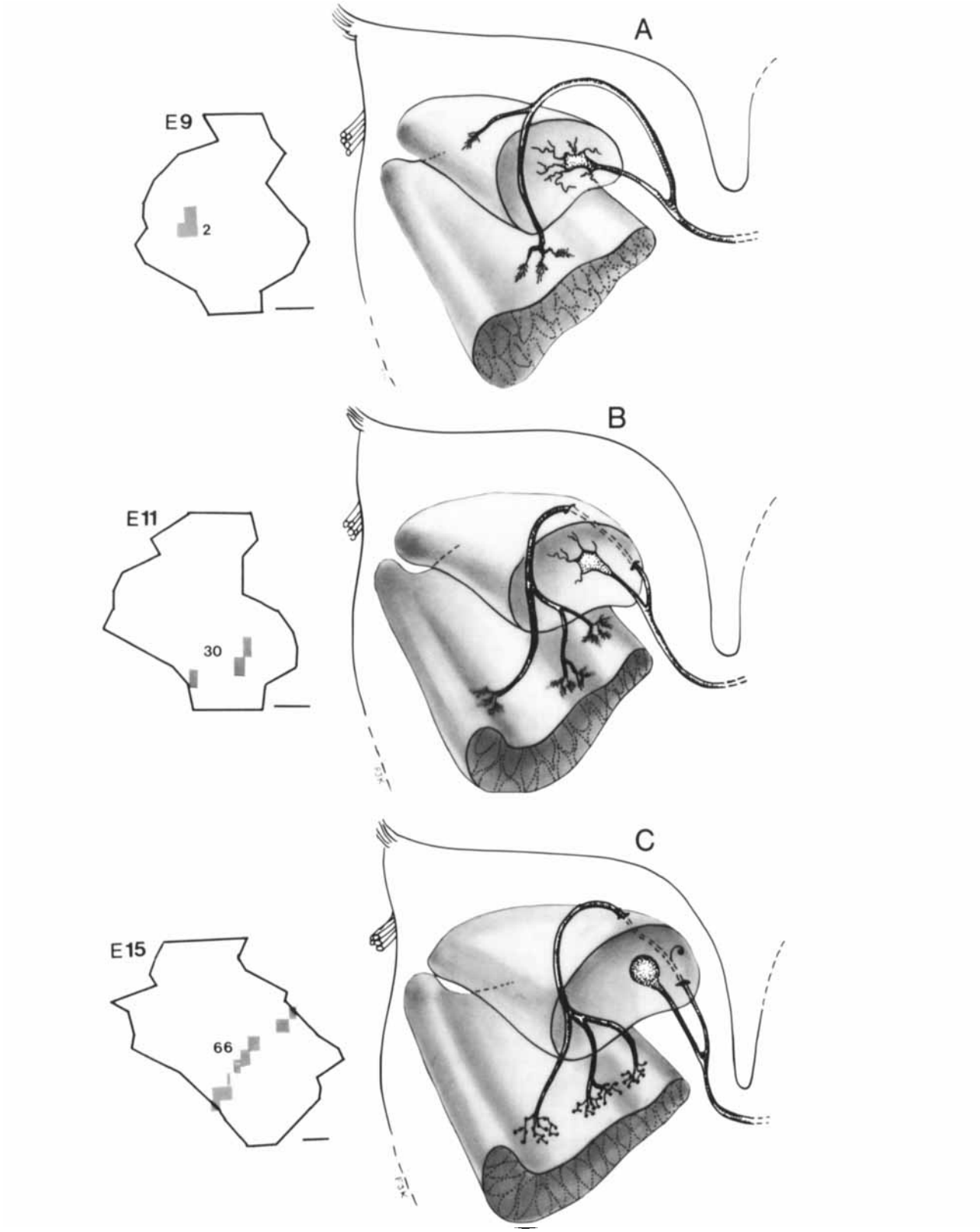

Fig. 20. Summary of changes in dorsal terminal arborizations between E9 and hatching. A from E9; B from E11; and C from E15. On the left are three representative planar projections showing a dorsal terminal field pattern at each of the ages indicated. On the right are schematic, three-dimensional drawings showing NM, NL, the axon trajectory, and the terminal arborization in NL. The drawings are viewed as if looking at the right side of the brain from the front. That is, medial is to the right, rostral is down and toward the viewer, and caudal is up and away. This orientation is best for viewing the entire trajectory of the axon. The planar projections are similarly oriented with rostral down and lateral to the left. The number on each planar projection refers to terminal field's number.

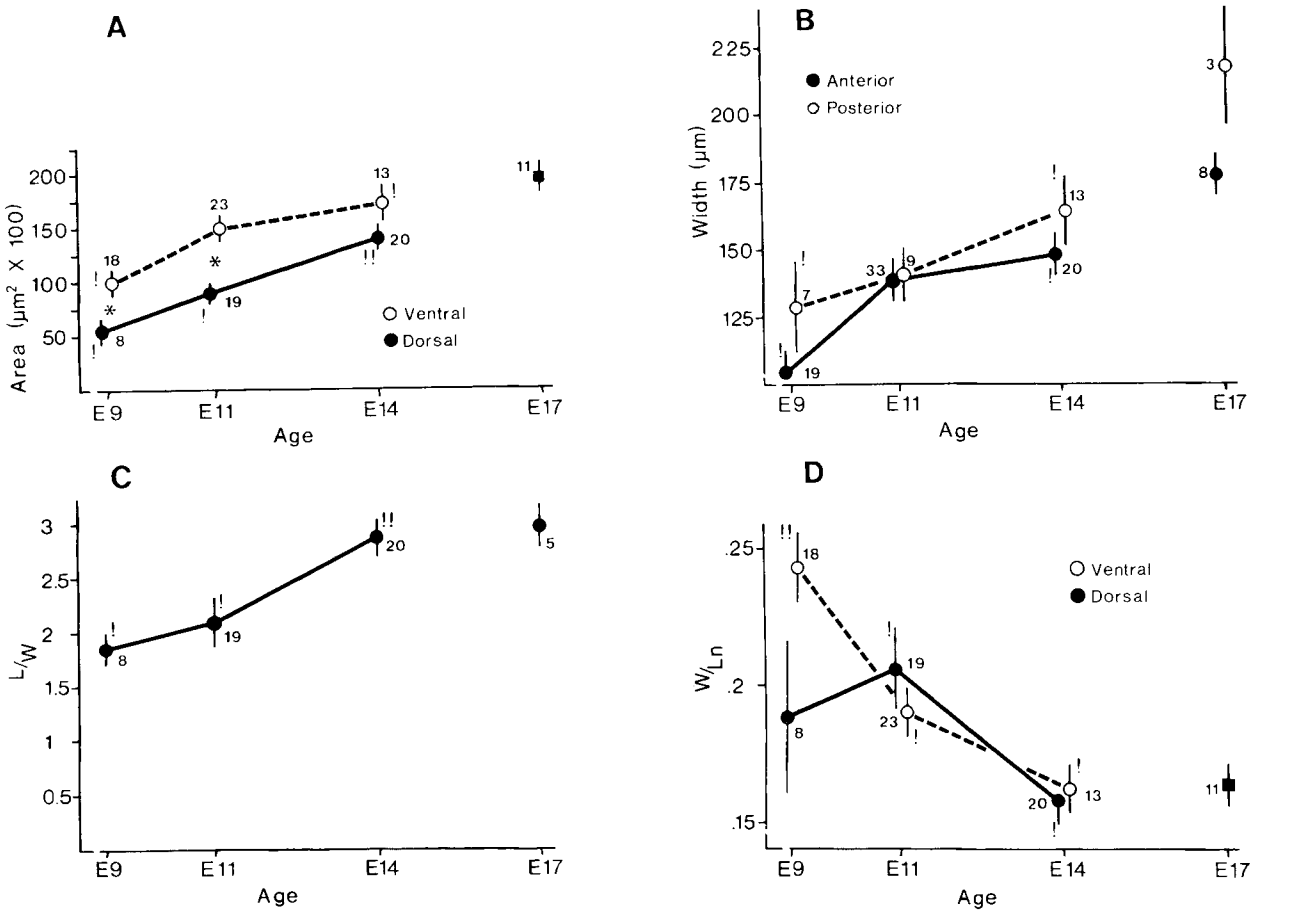

Fig. 21. A. Area of NM terminal field planar projections as a function of age and location on the dorsal and ventral side of NL. Open circles are data from ventral terminal fields; filled circles from dorsal terminal fields. The number of terminal fields represented by each point is indicated. Bars represent standard error of the mean. Statistical comparisons were made of groups, as shown, at E9, E9–E14, and E14–E17. Total area at E17 is also shown separately. Significant differences between individual groups ($P < .05$; Newman Keuls test) are indicated by * for dorsal and ventral groups at the same age and by ! for groups on the same side of NL at different ages. B. Anterior and posterior terminal field width as a function of age. Conventions are as in A. C. Dorsal terminal field L/W as a function of age. Length divided by width measures terminal field elongation (see Methods). Conventions as in A. (D). W/Ln of dorsal and ventral terminal fields as a function of age. Terminal field width was normalized by the length of the respective NL (see Methods). Conventions as in A.

Contralateral NM projection. A small percentage of NM axons branch near the medial edge of the contralateral NL and send a fiber dorsally into NM. These fibers are thin and may have a small terminal arbor (Fig. 29). Usually they terminate in the medial part of NM but occasionally they extend more laterally. One hundred four brains from E6 to E18 with HRP-filled axons numbering from one to over 100 were examined for this projection. About one brain in five had NM axon branches into the contralateral NM. Overall, we estimate that the frequency of this projection is less than 1%. It may be that they are more frequent in younger embryos but their rarity makes this point uncertain. Jackson and Parks ('84) have reported similar projections that occur much more frequently in chicks following unilateral otocyst ablation.

Cross lamina projections. Although most of an axon's terminal arborization is well restricted to the NL somata and the appropriate dorsal or ventral dendritic layer, a small number of branches cross the cell body layer and terminate on the opposite side of NL. These branches may also recross, sometimes leaving terminals in the inappropriate dendritic layer. Casual estimates suggest that about 5–10% of the terminals are in the dendritic layer opposite the main axon. No differences in this proportion were observed as a function of age.

Ipsilateral NM projection. A fourth type of aberrant NM projection will be described even though its origin has been positively identified in only one case. In our material at E17–E18 it is common to find small-caliber processes ending in large (3–5 μm) boutonlike structures that are stained with peroxidase reaction product and closely apposed to unstained NM somata (Fig. 30). To determine whether these are processes of HRP-filled NM neurons or are glial processes stained due to endogenous peroxidase, complete reconstructions of the fibers must be made. When TF 92 (Fig. 13) was reconstructed it was found to support one of these boutons on another NM neuron several hundred microns away (Figs. 13, 30B). Noncochlear inputs in NM have been described by Jhaveri and Morest ('82a) and by Parks ('81), but their source has not been identified. The identification of at least one of these fibers as belonging to an ipsilateral NM neuron suggests that additional experiments may identify a population of recurrent collaterals in NM.

NM dendritic development

NM cell bodies were themselves filled with HRP when their axons were injected. This made it possible to study the development of their dendritic arborizations as well as of their axons. The development of NM dendrites has already been described in detail by Jhaveri and Morest ('82a–c) on the basis of Golgi and electron microscope studies. Two points can be added to their descriptions.

Jhaveri and Morest describe the loss of elaborate somatic processes around embryonic day 15, but report no evidence of a spatial gradient in that loss. When HRP-filled neurons are observed over a wide extent of NM during this period, a clear gradient of dendritic loss is seen (Fig. 31). At E14, neurons in the rostromedial end of NM are completely bald, while caudolateral NM neurons still have profuse somatic processes. In younger embryos dendritic arborization is similar throughout NM and in later embryos all these neurons are adendritic.[1] Thus, the loss of somatic processes in NM occurs along a spatiotemporal gradient beginning rostromedially and ending caudolaterally. Smith ('81) and Parks and Jackson ('84) have made the same observation based on cells impregnated by the Golgi method and on HRP-filled cells. In addition, Figures 23 and 24 show that NM neurons with large, dendritelike processes often ending in growth cones are present as early as stage 29 (E6).

DISCUSSION

We have described two major organizational properties of the projection from n. magnocellularis (NM) to n. laminaris (NL). These properties are the ordered positions of the axon terminal fields and their elongated shapes, extending as patchy bands of terminals across NL.

The positional order of the terminal fields is the anatomical basis of the functional topography between NM and NL. It is demonstrated in dorsal NL by the correspondence of each NM cell's position with the position of its terminal field. Since the tonotopic axes in NM and NL are similar (Rubel and Parks, '75), this correspondence provides a qualitative indication of the appropriateness of the terminal field positions. Positional specificity could not be assessed by this method for the ventral terminal fields because they were separated from their somata by the injection procedure. Nevertheless, that their positions at E17 are similarly appropriate can be inferred from the tonotopy of the physiological responses at that age (Lippe and Rubel, '85).

The terminal fields' elongated shapes are probably related to temporal processing of binaural information (Young and Rubel, '83). Differences in arrival times of sounds at the two ears are important cues to the localization of sound in auditory space (Jeffress, '48; Galambos et al., '59; Goldberg and Brown, '69; Erulkar, '72; Jeffress, '75; Durlach and Colburn, '78; Colburn and Durlach, '78; Moiseff and Konishi, '83). The functional significance of the patchiness of terminals within each elongated terminal field is not understood.

The present developmental study shows that the two organizational properties, position and shape, are acquired in different ways by the dorsal and ventral terminal arborizations. The dorsal terminal fields are in appropriate positions at the time of their first elaboration in NL, not only along the NL frequency axis but across it as well. This second dimension of positional specificity may be due to developmental constraints, as it is not apparent at later stages. The initial shape of dorsal terminal fields, however, is far from mature. Several days are required to achieve the elongation initially present in the ventral terminal fields. Ventral terminal fields, on the other hand, are initially fully elongated but their position along the tonotopic axis appears to be less consistent initially and is subsequently adjusted, sometimes by substantial amounts, along the NL frequency axis. The developmental increase in frequency specificity (decreased W/Ln) for the terminal fields is also more apparent on the ventral side of NL.

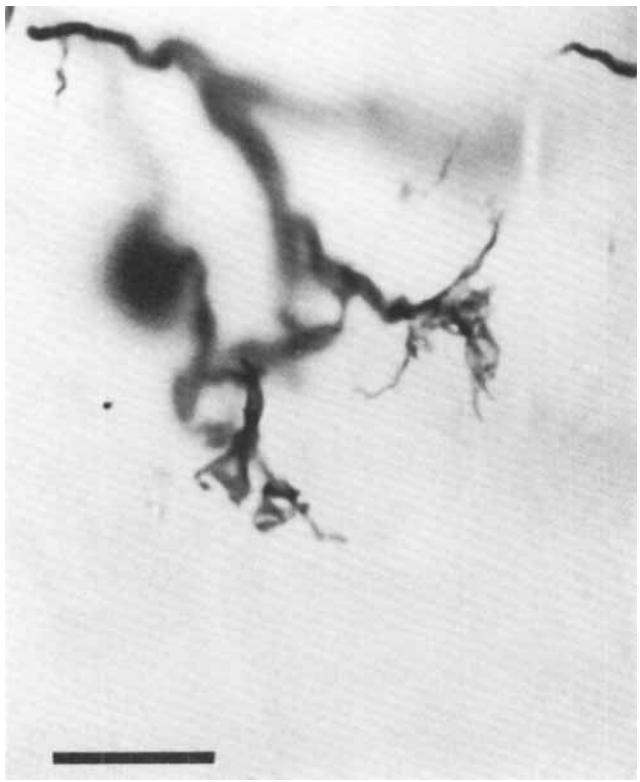

Fig. 22. Growing terminals in NL from ipsilateral NM cell at E8. NL has not yet developed its distinctive laminar organization and these growth cones are within the coalescing group of neurons. Bar = 10 μm.

The shift in ventral terminal field positions was suggested by the observation that at E14–17 many ventral terminal fields are dislaced from their axons, while in younger chicks ventral axons are always closely associated with their terminal fields. That this displacement involves a real shift in terminal field position was confirmed by the observation that terminal fields that must have been coextensive at earlier stages, because their main axons were intertwined, had completely separated by E17. It might be argued that the axons with displaced terminal fields grew into NL later than other axons but this is ruled out by the fact that fully half of the terminal fields at E14–E17 are displaced and show no evidence of less mature terminal morphology. Another possibility is that movement of the

[1] It should be noted that neurons in the ventrolateral division of NM, which are not auditory but lagenar (Boord, '69), do not participate in this process and do not lose their early dendritic arborization. None of these neurons was included in this study, though their axonal arborizations are basically similar to those of neurons in NM proper (i.e., NM medialis and NM lateralis; Boord, '69; Jhaveri and Morest, '82a).

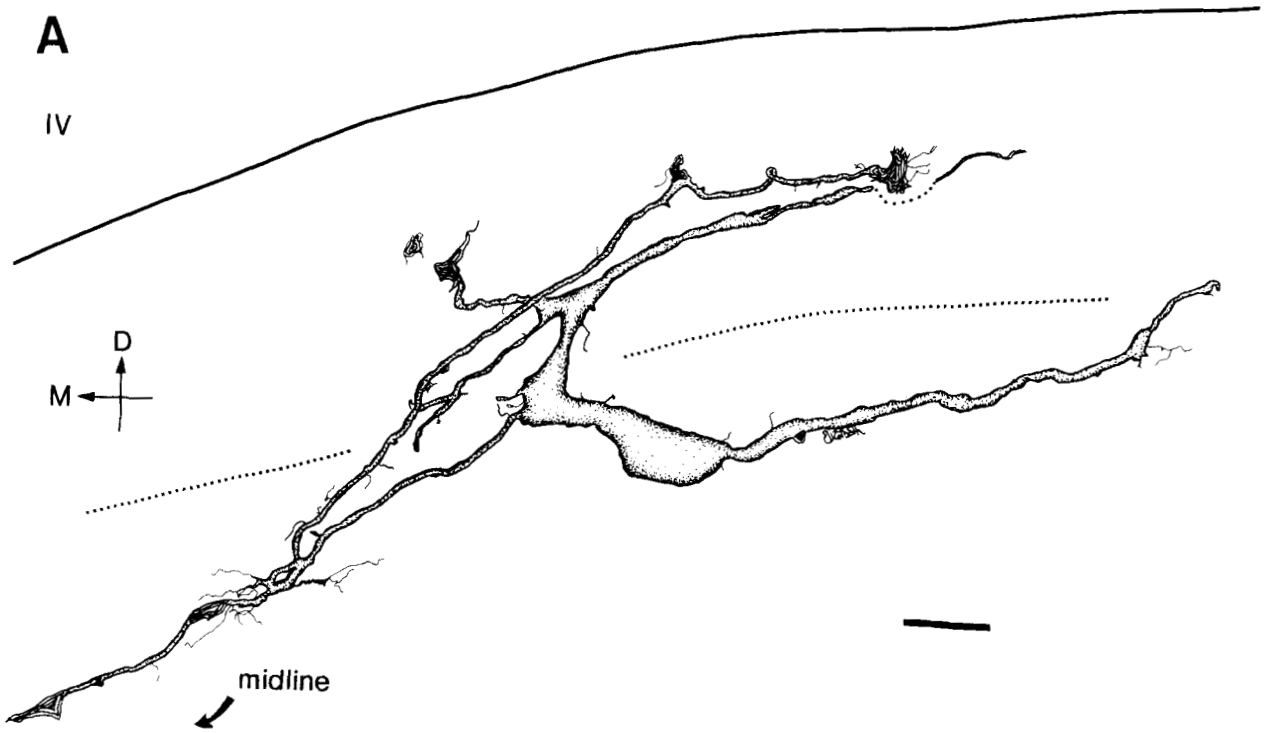

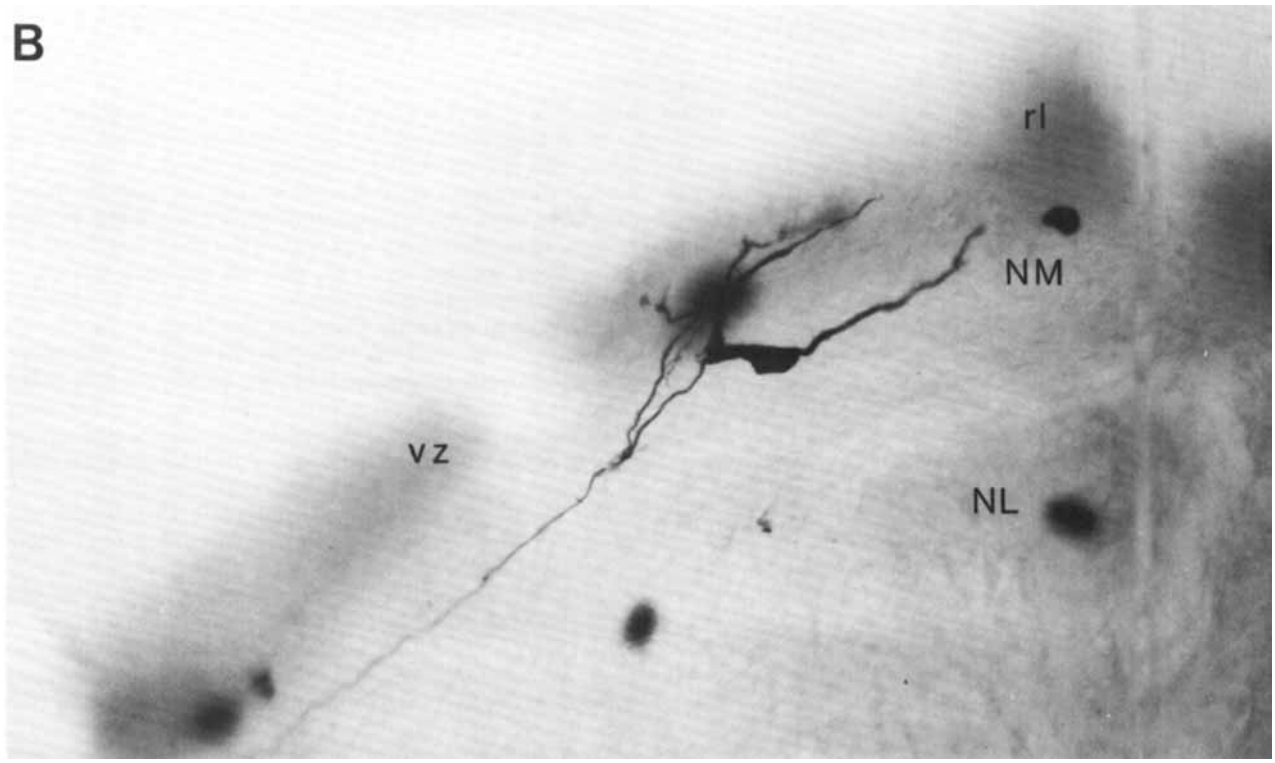

Fig. 23. A. Camera lucida drawing of the neuron shown in B. The lower edge of the ventricular zone is indicated by the dotted line. B. Photomicrograph of an HRP-filled NM neuron at E6. The ventricular proliferation zone, VZ, is the darker layer along the dorsomedial surface of the section. It ends at the upturned rhombic lip, rl, dorsolateral to the stained neuron. This is the first stage at which clumps of cells corresponding to NM and NL can be distinguished from each other. The rounded black masses are red blood cells. IV is the fourth ventricle, D dorsal, M medial. Bar = 10 μm in A.

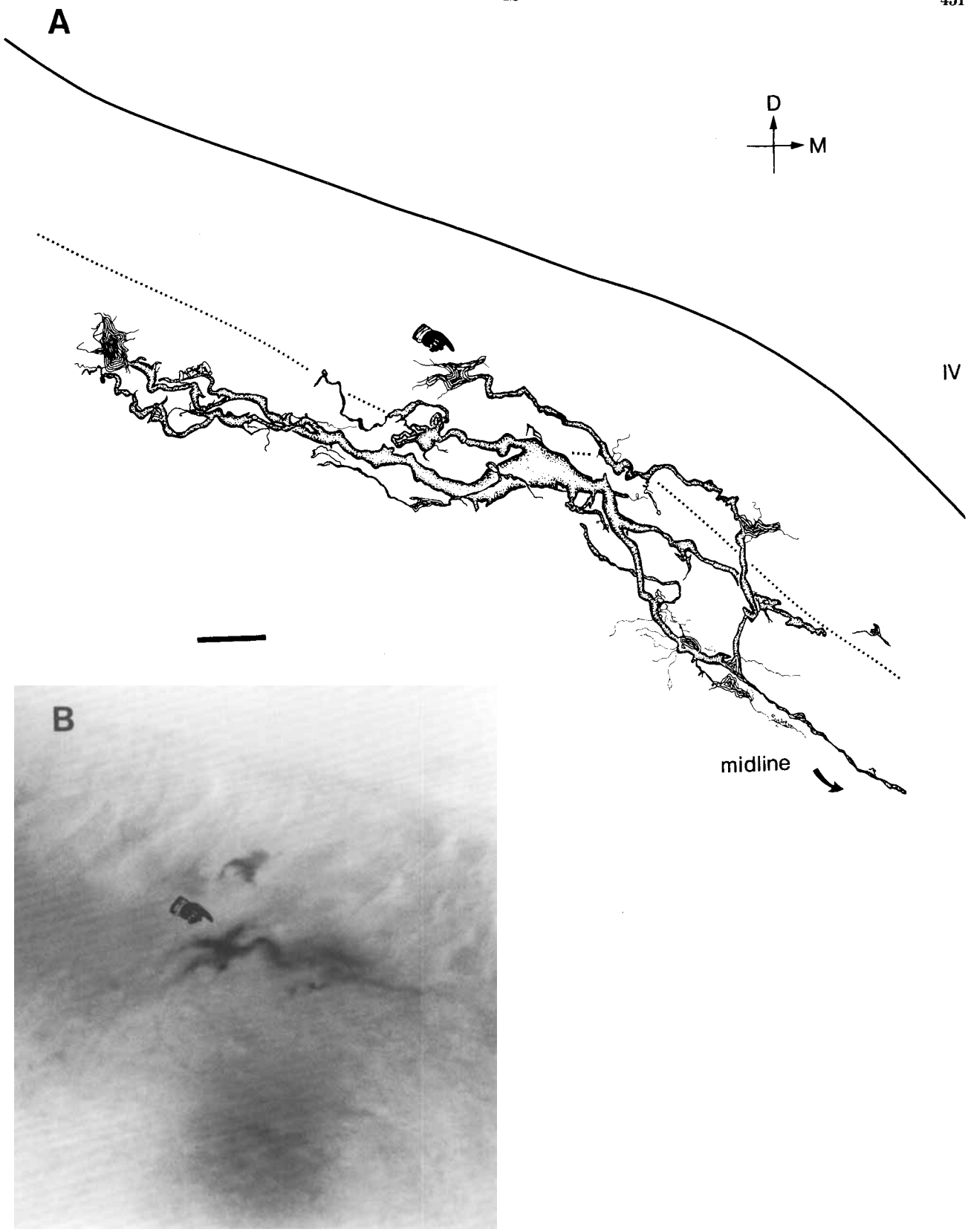

Fig. 24. A. Camera lucida drawing of an HRP-filled NM neuron on the opposite side of the same brain shown in Figure 23. A large growth cone can be seen at the end of the laterally directed neurite. The bottom edge of the ventricular zone is indicated by the dotted line. The growth cone in the ventricular zone at the end of the ipsilateral axon branch (pointer) is shown enlarged in the photomicrograph in B. Bar = 10 μm.

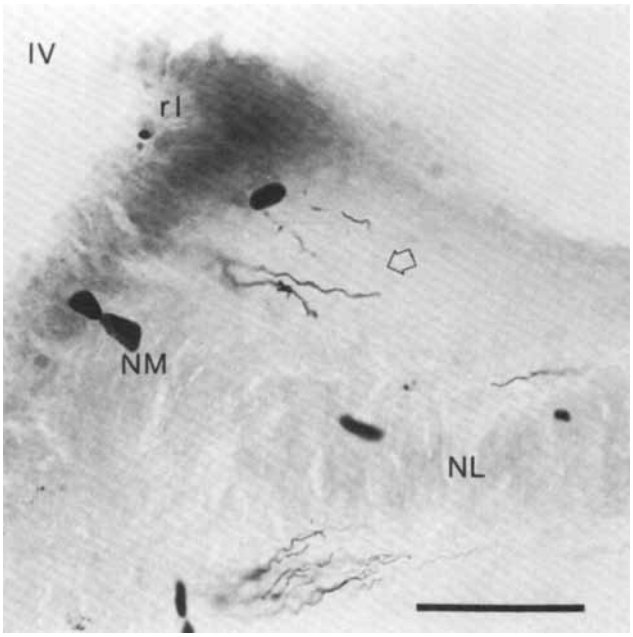

Fig. 25. Photomicrograph of dorsolateral brain stem at E7. IV is the fourth ventricle. A few HRP-stained NM axons (open arrow) can be seen growing toward NL from the ventricular zone. Several stained NM axons from the contralateral side can also be seen at the ventromedial border of NL. Round black masses are red blood cells. Dorsal is up, medial to left. rl, rhombic lip; nm, nucleus magnocellularis; nl, nucleus laminaris. Bar = 50 μm.

target cells accounts for the terminal field shifts. Since approximately 75% of NL neurons die betwen E11 and E13 (Rubel et al., '76) this possibility cannot be ignored. Nevertheless, when it is considered that ventral terminal fields move as units, remaining elongated across NL at all times; that they move in opposing directions and by different amounts; and finally, that no comparable shifts occur in the positions of the dorsal terminal fields, this hypothesis also appears untenable. It seems most likely that between E11 and E14 the growing ventral arbors sprout and retract fine processes to sample their target choices in NL, maintaining preferentially the more appropriate connections, and finally occupy positions at or to either side of their original sites. Other instances of continuous developmental shifts in terminal field positions have been reported in the retinotectal projections of frogs (Reh and Constantine-Paton, '85), goldfish (Easter and Stuermer, '84) and chicks (McLoon, '85), and in the isthmotectal projection of frogs (Udin, '84). There is also evidence that an auditory map in the optic tectum of owls shifts in response to changing binaural spatial cues during development (Knudsen, '85). Thus, the finding of developmental terminal field shifts in NL cannot, in itself, be regarded as novel, although the terminal field shifts of the retinal axons seem to be involved with in-register shifts of the visual map as a whole rather than with actual establishment of the topographic order, as in NL.

In summary, position is an original property of the dorsal terminal fields, and elongation (derived from the path of the contralateral axon coursing beneath the presumptive NL) originates with the ventral arborization. The similari-

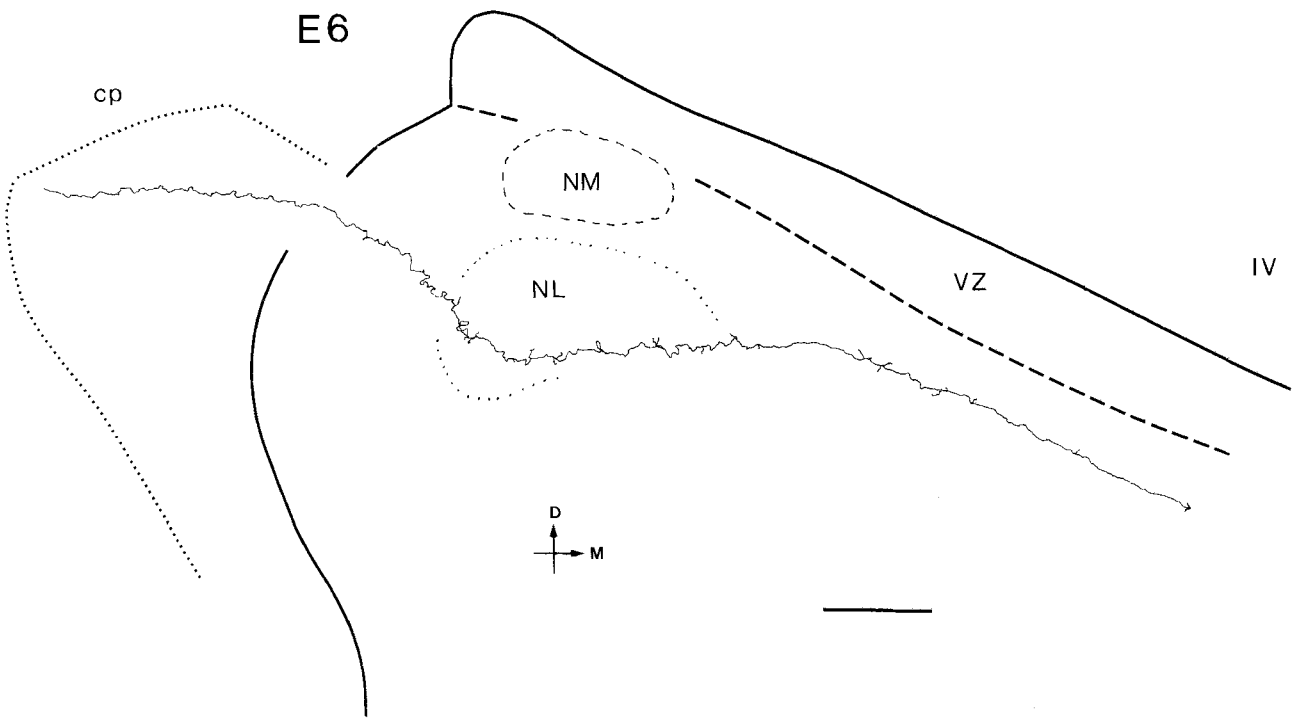

Fig. 26. Camera lucida reconstruction of ventral axon from the contralateral NM coursing through NL at E6. This axon was traced 200–300 μm rostral to NL until it was lost at the cut stump of the cerebellar peduncle (cp). The brainstem outline at that anterior level is shown by the dotted line. IV, fourth ventricle; VZ, ventricular zone; NL, nucleus laminaris; NM, nucleus magnocellularis. Dorsal is up, medial to the right. Bar = 50 μm.

Fig. 27. Photomicrograph of one-half coronal section of chick hindbrain at E9. The remainder of the cerebellum was removed when the brainstem was explained. This section is 600 μm rostral to the anterior pole of NL. The area between the arrows is the site of termination of at least some of the anterior projections of the contralateral NM axon branches. M, midline at fourth ventricle. Bar = 0.5 mm.

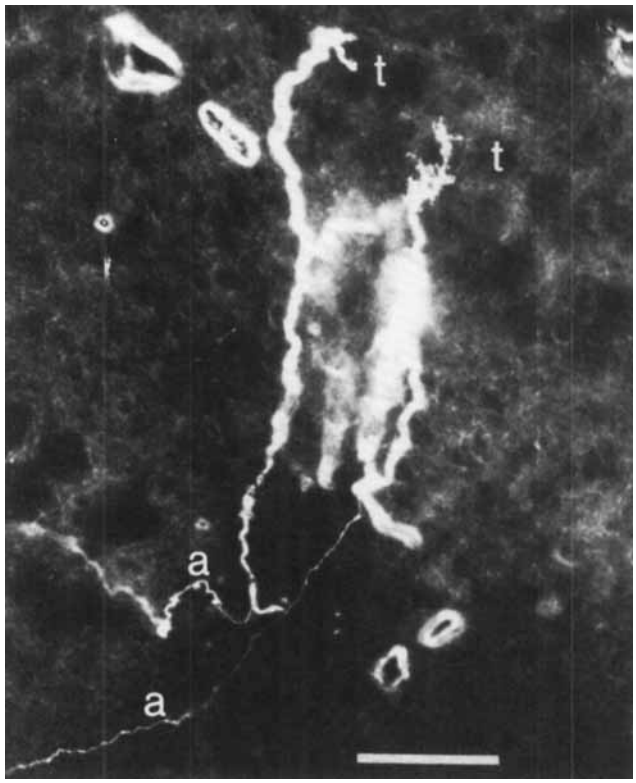

Fig. 28. Darkfield photomicrograph of the antero-lateralmost terminal clusters, t, of two ventral NM axons in anterior NL. The thin fibers at the lower left, a, are the beginnings of the long anterior fibers that continue into the cerebellar penduncle from the ventral NM axon at early stages; 11-day embryo. Bar = 20 μm.

ties between dorsal and ventral terminal fields—the elongation of dorsal terminal fields and the final positions of the ventral arborizations—are acquired during subsequent development.

Convergence of dorsal and ventral terminal field patterns

Between E9 and E14 terminal field reorganization occurs, during which each set of afferents acquires the organizational property that originated in the other. Concomitantly structural and functional synaptogenesis occurs (Saunders et al., '73; Jackson and Rubel, '78; Jackson et al., '82; Jhaveri and Morest, '82c).

The developmental changes in NM terminal morphology that occur during this period are consistent with a role for activity in the terminal field reorganization. From E8 through E11, when the dorsal terminal fields are beginning to elongate and the ventral arborizations are becoming more complex, veiled terminals resembling growth cones are common in NL neuropil. Argiro et al. ('84) found that the rate of extension of growth cones in culture decreased when lamellipodia were replaced by the more adherent filopodia. In NL the frequency of veiled endings decreases as the axons achieve their greatest elaboration of fine processes. This profusion of extremely fine filopodialike processes ramifying densely in the NL neuropil reaches its peak on E11–E12, and is matched by "a great profusion of fine dendritic or filopodial processes" (Smith, '81). E11–E12 is also the time at which postsynaptic responses can first be elicited in NL by stimulation of the auditory nerve (Jackson et al., '82), and it may be that these fine axonal and dendritic processes are the sites of the primitive synaptic contacts. Between E14 and E17, when the elongation of the dorsal terminal fields (L/W) and the frequency specificity (W/Ln) of all the terminal fields have reached plateaus, most of these fine processes are lost and the axons develop large boutons. This may correspond to the elimination and consolidation of exuberant synapses described by many authors (e.g., Atsumi, '77; Lichtman, '77; Lichtman and Purves, '80; Smolen and Raisman, '80; Johnson and Purves, '81; Jackson and Parks, '82; Shatz and Kirkwood, '84; Sretavan and Shatz, '86). It is important to note that the sequence of changes in ending morphology that we have observed is consistent with previous observations using both HRP and Golgi methods (Ramón y Cajal, '60; Morest, '68; Mason, '82, '85; Mason and Gregory '84). There appear to be some general rules: (1) lamellipodia with many filopodia are found at choice points; (2) elongated lamellipodia with few filopodia are found where there is directed rapid growth; (3) the delicate profusion of dense filopodialike pro-

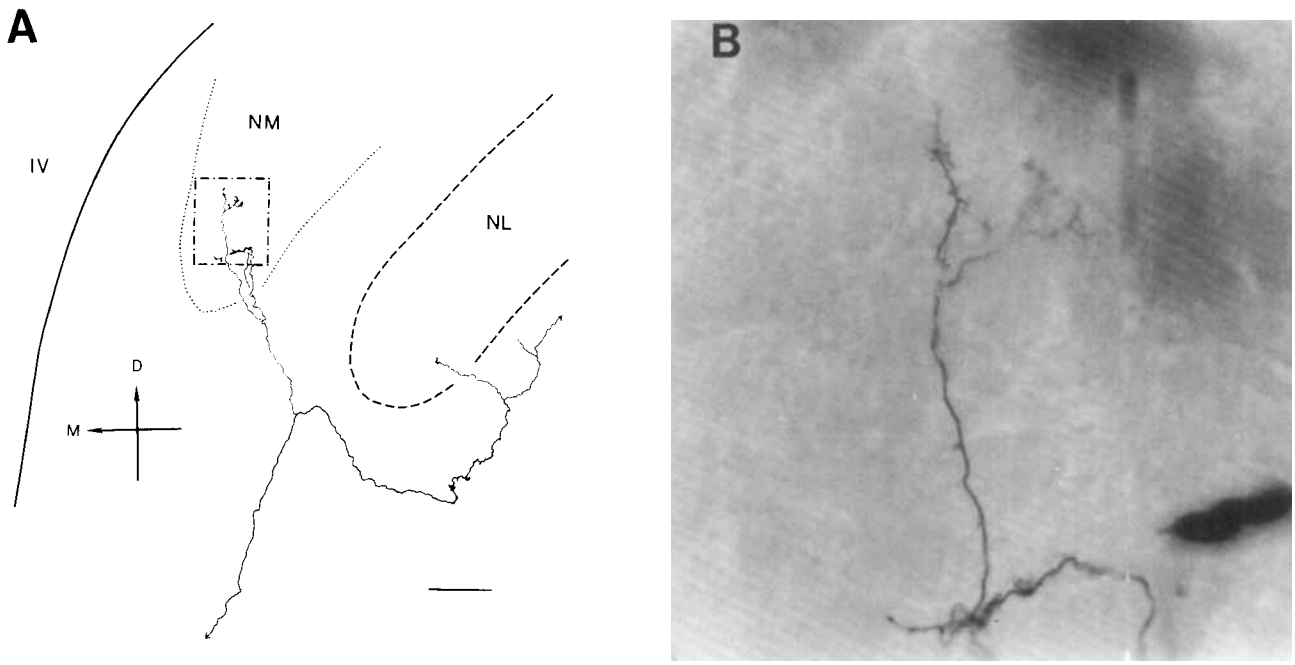

Fig. 29. Branch of an NM axon with a cluster of terminals in the contralateral NM. These branches are very rare in normal chicks (see text); 11-day embryo. A. Reconstruction of medial end of contralateral NM axon arborization. Axon has typical arborization in ventral NL neuropil as well as branch coursing dorsally into NM. Conventions as in Figure 3. Bar = 50 μm. B. Photomicrograph of the terminal cluster outlined in A. Oblong dark mass is red blood cells.

cesses is an early characteristic of axons reaching their target region; and (4) the elimination or coalescing of fine branches into definitive boutons is the final stage of maturation and associated with the development of physiological function.

If coincident pre- and postsynaptic activity tends to stabilize the synapse (Hebb, '49; Hubel and Wiesel, '65; Stent, '73; Stryker, '82; Stryker and Harris, '86; Sanes and Constantine-Paton, '85; Reh and Constantine-Paton, '85; Schmidt, '85; but see Ross and Godfrey, '84; and Tumosa et

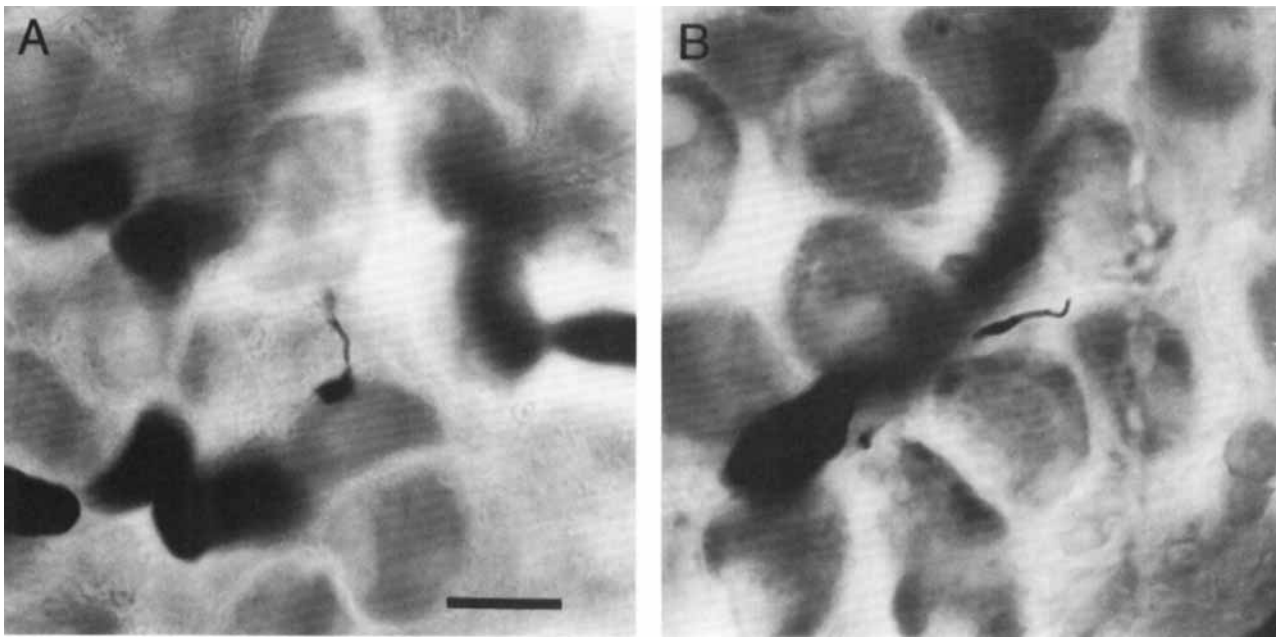

Fig. 30. Boutons in E17 NM stained with peroxidase reaction product; sections were counterstained with toluidine blue. Rounded black masses are red blood cells. Dorsal is up, medial to right. Bar = 10 μm. A. Bouton and fiber that parallel the course taken by the fiber shown in B, but that could not be traced to its parent soma. Similarly stained boutons are common in NM at E17. B. Cross section of an HRP-stained bouton traced to TF 92 (drawn in Fig. 13).

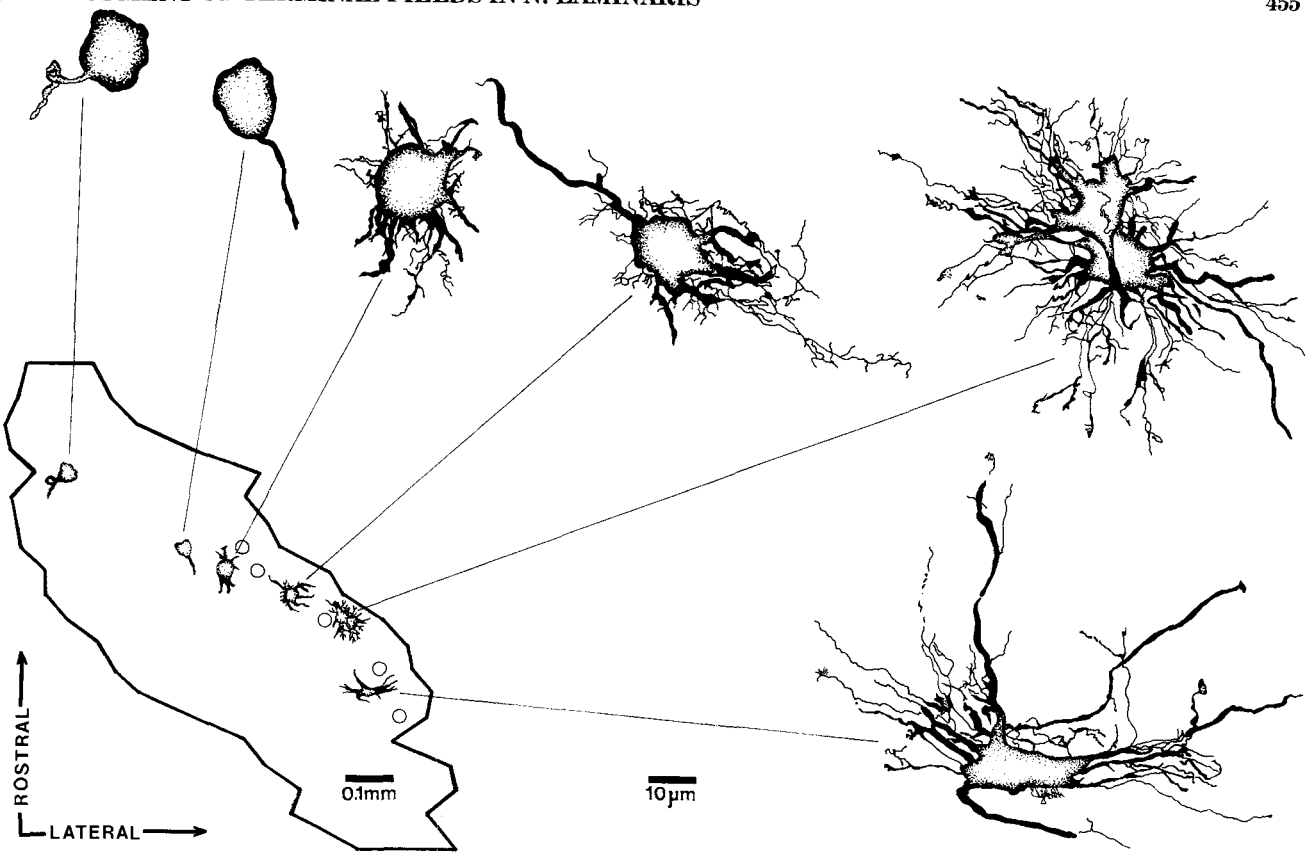

Fig. 31. Planar projection of NM and camera lucida drawings of NM cells at the indicated locations in NM at E14.

al., '84), then terminal fields carrying similar information to the two sides of NL should naturally come to resemble each other. The more highly ordered dorsal terminal fields might be more effective in driving NL neurons, and the ventral terminal fields would shift in order to match frequency response characteristics. At the same time, the dorsal terminal fields would maximize their coverage of coactive NL neurons by extending along the orientation already established by the ventral terminal fields. This hypothesis implies that alignment of dorsal and ventral terminal fields is dependent on the normal coordination of activity to the two sides of NL. Failures of normal synaptic reorganization resulting from an imbalance of activity have been reported by several authors (Benoit and Changeux, '78; Srihari and Vrbova, '78; Hubel et al., '77; Shatz and Stryker, '78; Rakic, '81; Stryker, '81; Stryker and Harris, '86).

Many reports of synaptic reorganization during development describe a reduction in divergence or the segregation of inputs from different sources (Redfern, '70; Brown et al., '76; Lichtman and Purves, '80; Lichtman, '77; LeVay et al., '78; Bentley and Toroian-Raymond, '81; Jackson and Parks, '82; Wallace, '84; Heathcote and Sargent, '85; Sretevan and Shatz, '86). NM axons also reduce the *relative* size of their termination but not the *absolute* size of the arborization (Fig. 21). Similar findings are reported by Sretevan and Shatz ('86) and by Sakaguchi and Murphey ('85). However, the primary effect of the reorganization in NL is to pull the already segregated dorsal and ventral terminal fields into comparable positions and orientations with respect to the tonotopic axis.

Origins of initial terminal field patterns

We have attempted to explain how two characteristics of the NM terminal field pattern, position and shape, are established during the terminal field reorganization between E9 and E14. It would be particularly satisfying to trace these characteristics one step further toward their sources and to discover how each comes to be an initial property of one set of terminal fields. In the case of the ventral terminal fields, their elongated shape appears to be a simple consequence of the anterolaterad course of the early contralateral axon ventral to and beyond NL. The E6 contralateral axon branch takes a fairly direct course medially from its cell body and then laterally beyond the midline, following the ventral border of the ventricular layer until turning rostrolaterally in the region of the contralateral NL. The border of the ventricular zone might be a permissive region for axon growth (as described by Tosney and Landmesser, '84, for motor axons in the chick hindlimb). If so, the nature of the conditions that restrict growth outside this region or of the signal that directs the axons rostrally when they have reached their target remains a mystery. In any case, the transient projection of the contralateral branch toward the cerebellum suggests the possibility that the contralateral axon's path with respect to NL may be incidental to its course toward a more rostral target.

The course of the dorsal NM axon prior to E9 suggests an interesting possibility regarding the ontogenesis of the topographic precision between NM and the ipsilateral NL. Some background information is required. NM and NL neurons are born near the rhombic lip just dorsal to their

site in Figure 23A (Huggosson, '57). The "birthdays" of NM and NL neurons are different and nonoverlapping—NM neurons undergoing their final mitoses between 60 and 72 hours of incubation, and NL between 84 and 108 hours (Rubel et al., '76). The NL cells then migrate past the existing NM neurons and can be observed first coalescing ventral to NM on E6 (Huggosson, '57). Yet at E6 the growing tip of the ipsilateral NM axon branch is not directed toward the NL cells ventral to NM. Instead, the ipsilateral growth cone is among or adjacent to the dividing cells in the ventricular zone.

The obvious implication of this observation is that the closest target of the earliest ipsilateral branch of the NM axon is not ventral to NM. Rather, when the axon first begins to grow, its ipsilateral target is in the ventricular zone. Given that NL neurons are born in E4–E5 in the same area occupied by NM growth cones at E6, it must be suggested that at E6 either some premigratory NL neurons or the trailing processes of migrating NL cells are still present in the ventricular layer. At E5–E6 the NM neuron is no more than 50 μm from its appropriate premigratory targets and these targets could be identified by filopodia growing at random from the NM soma or axonal growth cone. Since the ipsilateral axon's arborization in dorsal NL is already appropriately positioned at E9, we suggest that the initial association of the growth cone with an NL cell (or cells) in the ventricular layer is also quite specific. Neuronal pathway selection by this means has been described in the embryonic grasshopper leg by Keshishian and Bentley ('83a–c) and by Ho and Goodman ('82). The loop formed by the ipsilateral NM axon branch is completed by the axon following or being towed by its migrating target into NL. We have no evidence that suggests any particular mechanism for this early specificity. However, recent evidence that neurons can form connections on the basis of cell-specific identities has been reported by Purves et al. ('81), Wigston and Sanes ('82), and Raper et al ('83a,b). The simplest possibility is that those NM and NL neurons that become connected were generated at the same site.

In order for specific connections between growth cones and targets in the ventricular layer to be translated into specific terminal field positions in dorsal NL neuropil, specifically guided migrations of the target NL cells must also occur. Occasional radially arranged glial cells are stained in our material by an endogenous peroxidase. Radial glial fibers might provide a highly ordered scaffolding for NL migration, as has been shown by Rakic ('72, '77a) for neurons in other parts of the brain. It would be of great value to know if the migration patterns of NL neurons actually do reflect the sites or timing of their generation in the ventricular layer.

The hypothesis that specific connections are made before migration of the target cells is completed may have widespread applicability. Morest ('69, '70) has shown that presynaptic axons could make contact with the leading or trailing processes of migrating neurons. Rakic ('77b) stresses that fiber tracts are a prominent feature of the intermediate zone of the embyronic forebrain and suggests that the axons appear to be waiting for their migrating targets to pass among them. Other examples can be identified where neuronal populations that form precise topographic connections over long distances are thought to arise from adjacent or nearby germinal sites. For example, Harkmark ('54, '56) reported that cells of the inferior olive migrate from a dorsolateral position on the rhombic lip, a site very close to the germinal site of cerebellar Purkinje cells. Similarly, Huggosson ('57) indicates that cells of the superior olive originate near neurons that will differentiate into the cochlear nucleus. In both of these examples the question remains open as to when the first contacts are actually made. Furthermore, a recent report by Metcalfe ('85) shows that ganglionic neurons and sensory receptor cells of the zebrafish posterior lateral line arise from adjacent areas of a common placode in the caudal head region. HRP filling of ganglion cells revealed that growth cones entered the premigratory sensory primordium and remained associated with it during its caudal migration along the body. As sensory cells are deposited they are innervated by some of the associated axons.

Dorsal/ventral polarity of NL

On E5–E6, axons from the contralateral NM have reached the presumptive site of NL. It is attractive to hypothesize that these early contralateral axons could provide the signal that stops migration of the NL neurons. This hypothesis predicts that absence of the contralateral NM axons would adversely affect NL migration, perhaps in the same way that absence of the eighth nerve fibers abnormally prolongs the migration of neurons in nucleus angularis (Parks, '79). Preliminary evidence suggests that preventing growth of the contralateral axons across the midline severely disrupts migration and lamination of the NL neurons (Moody and Rubel, unpublished observations).

It may be further suggested that the dorsal/ventral polarity of NL dendrites is established during migration. The initial contacts of the contralateral NM axon with the leading process of the migrating NL neuron and of the ipsilateral axon branch with the trailing NL process could serve this purpose. Since some NM terminals normally occur in the inappropriate NL neuropil layer, the only mechanism that needs to be invoked for segregating dorsal and ventral afferents to NL is the earlier presence of the appropriate terminals. In fact, Rubel et al. ('81) found that if the balance of input to the two NL dendrites is disrupted, sprouting can occur from the remaining afferents to the "wrong dendrite."

CONCLUSION

The results of this study are consistent with the view that specific neural connections are formed by a process consisting of at least two stages (LeVay et al., '75; Rakic, '77b; Law and Constantine-Paton, '81; Constantine-Paton et al., '83; Meyer, '83; Reh and Constantine-Paton, '84; Tosney and Landmesser, '84; Easter et al., '85). In the first stage highly directed axon growth results in most axons reaching their target region with very few errors (Landmesser, '78; Hollyday, '83; Rubin, '85a,b; Sakaguchi and Murphey, '85). In this stage axons appear to make use of whatever mechanical and chemical cues are available at a given time (Lance-Jones and Landmesser, '80; Flaster et al., '82; Reh et al., '83; Raper et al., '83a,b; Harris, '84; Tosney and Landmesser, '84). In the present paper, highly directed axon growth is shown by the positional specificity of the earliest terminal fields in the dorsal NL neuropil. A clue to its mechanism may be the specific association of the ipsilateral NM growth cone with presumptive NL cells in the ventricular zone.

During a second stage, connections are reorganized by a mechanism that may depend on activity (see above). As yet, there is no direct evidence for a role of activity in guiding the reorganization of NM terminal fields, but the temporal

correspondence of this reorganization with synapse formation and the onset of auditory function strongly suggests that the two initially discrepant projections become similar as a result of activity-related events.

Another implication of this study is that reorganization of terminal arborizations is not limited to quantitative adjustments and sharpening of preexisting patterns (Purves and Lichtman, '85: Chapter 12). During terminal field reorganization in NL, a new pattern of connections emerges that embodies the major preexisting pattern of both the dorsal and the ventral elements. Creation of new synaptic patterns by the combination and reorganization of preexisting patterns could be an important developmental strategy and might be more frequently observed as the development of complex central synaptic patterns comes under increasing scrutiny.

ACKNOWLEDGMENTS

We would like to thank Dr. Sally Moody for long discussions over the microscope, Dr. Lynne Olsho for help with the quantitative comparisons, and Elizabeth Cantrell for some of the drawings. Drs. Jeremy Tuttle, Otto Friesen, Michael Merickel, Oswald Steward, Theodore Rall, Peter Brunjes, Leonard Kitzes, Dianne Durham, William Lippe, Richard Hyson, Dan Sanes, Kenneth Muller, Carol Mason, and David Sretavan provided valuable comments on earlier versions of the manuscript. Sharon Davis provided typing and editorial help. We would especially like to thank Patricia Palmer, whose treatment of the histological sections faithfully revealed their great natural beauty. The data were presented by S.R.Y. in partial fulfillment of the Ph.D. degree requirements of the University of Virginia. This work was supported by NINCDS grant number NS 15478 and funds from the Lions of Virginia Hearing Foundation.

LITERATURE CITED

Adams, J.C. (1981) Heavy metal intensification of DAB-based HRP reaction product. J. Histochem. Cytochem. *29:*775.

Argio, V., M.B. Bunge, and M.I. Johnson (1984) Correlation between growth form and movement and their dependence on neuronal age. J. Neurosci. *4:*3051–3062.

Atsumi, S. (1977) Development of neuromuscular junctions of fast and slow muscles in the chick embryo: A light and electron microscopic study. J. Neurocytol. *6:*691–709.

Benoit, P., and J.-P. Changeux (1978) Consequences of blocking the nerve with a local anesthetic on the evolution of multiinnervation at the regenerating neuromuscular junction of the rat. Brain Res. *149:*89–96.

Bentley, D., and A. Toroian-Raymond (1981) Embryonic and postembryonic morphogenesis of a grasshopper interneuron. J. Comp. Neurol. *201:*507–518.

Boord, R.L. (1969) The anatomy of the avian auditory system. Ann. N.Y. Acad. Sci. *167:*186–198.

Boord, R.L., and H.J. Karten (1974) The distribution of primary lagenar fibers within the vestibular nuclear complex of the pigeon. Brain Behav. Evol. *10:*228–235.

Brown, M.C., J.K.S. Jansen, and D. Van Essen (1976) Polyneuronal innervation of skeletal muscle in new-born rats and its elimination during maturation. J. Physiol (Lond.) *261:*387–422.

Colburn, H.S., and N.I. Durlach (1978) Models of binaural interaction, Chapter 11. In E.C. Carterette and M.P. Friedman (eds): Hearing, Vol. IV of Handbook of Perception. New York: Academic Press. pp 467–518.

Constantine-Paton, M., E.C. Pitts, and T.A. Reh (1983) The relationship between retinal axon ingrowth, terminal morphology, and terminal patterning in the optic tectum of the frog. J. Comp. Neurol. *218:*297–313.

Durlach, N.I., and H.S. Colburn (1978) Binaural phenomena, Chapter 10. In E.C. Carterette and M.P. Friedman (eds): Hearing, Vol. IV of Handbook of Perception. New York: Academic Press. pp 365–466.

Easter, S.S., D. Purves, P. Rakic, and N.C. Spitzer (1985) The changing view of neural specificity. Science *230:*507–511.

Easter, S.S., Jr., and A.O. Stuermer (1984) An evaluation of the hypothesis of shifting terminals in goldfish optic tectum. J. Neurosci. *4:*1052–1063.

Erulkar, S.D. (1972) Comparative aspects of spatial localization of sound. Physiol. Rev. *52:*237–360.

Flaster, M.S., E.R. Macagno, and R.S. Schehr (1982) Mechanisms for the formation of synaptic connections in the isogenic nervous system of daphnia magna. In N. Spitzer (ed): Neuronal Development. New York: Plenum Press.

Galambos, R., J. Schwartzkopff, and A. Rupert (1959) Microelectrode study of superior olivary nuclei. Am. J. Physiol. *197:*527–536.

Goldberg, J.M., and P.B. Brown (1969) Response of binaural neurons of dog superior olivary complex to dichotic tonal stimuli: Some physiological mechanisms of sound localization. J. Neurophysiol. *32:*613–636.

Hackett, J.T., H. Jackson, and E.W. Rubel (1982) Synaptic excitation of the second and third order auditory neurons in the avian brain stem. Neuroscience *7:*1455–1469.

Hamburger, V., and H.L. Hamilton (1951) A series of normal stages in the development of the chick embryo. J. Morphol. *88:*49–92.

Harkmark, W. (1954) Cell migrations from the rhombic lip to the inferior olive, the nucleus raphe and pons. A morphological and experimental investigation on chick embryos. J. Comp. Neurol. *100:*115–209.

Harkmark, W. (1956) The influences of the cerebellum on development and maintenance of the inferior olive and the pons. J. Exp. Zool. *131:*333–371.

Harris, W.A. (1984) Axonal pathfinding in the absence of normal pathways and impulse activity. J. Neurosci. *4:*1153–1162.

Harrison, R.G. (1910) The outgrowth of the nerve fiber as a mode of protoplasmic movement. J. Exp. Zool. *9:*787–846.

Heathcote, R.D., and P.B. Sargent (1985) Loss of supernumerary axons during neuronal morphogenesis. J. Neurosci. *5:*1940–1946.

Hebb, D.O. (1949) Organization of Behavior. New York: John Wiley and Sons.

Ho, R.K., and C.S. Goodman (1982) Peripheral pathways are pioneered by an array of central and peripheral neurons in grasshopper embryos. Nature *297:*404–406.

Hollyday, M. (1983) Development of motor innervation of chick limbs. In J.F. Fallon and A.I. Caplan (eds): Development and Regeneration, Part A. New York: Alan R. Liss, Inc., pp. 183–93.

Hubel, D.H., and T.N. Wiesel (1965) Binocular interaction in striate cortex of kittens reared with artificial squint. J. Neurophysiol. *28:*1041–1059.

Hubel, D.H., T.N. Wiesel, and S. LeVay (1977) Plasticity of ocular dominance columns in monkey striate cortex. Philos. Trans. R. Soc. Lond. [Biol.] *278:*377–409.

Huggoson, R. (1957) Morphologic and Experimental Studies on the Development and Significance of the Rhombencephalic Longitudinal Cell Columns. Translated from Swedish by Victor Braxton. Lund: Hakan Ohlssons Boktryckeri.

Jackson, H., J.T. Hackett, and E.W. Rubel (1982) Organization and development of brain stem auditory nuclei in the chick: Ontogeny of postsynaptic responses. J. Comp. Neurol. *210:*80–86.

Jackson, H., and T.N. Parks (1982) Functional synapse elimination in the developing avian cochlear nucleus with simultaneous reduction in cochlear nerve axon branching. J. Neurosci. *2:*1736–1743.

Jackson, H., and T.N. Parks (1984) Development of a novel projection to the avian cochlear nucleus following otocyst removal. Soc. Neurosci. Abstr. *297:*5.

Jackson, H., and E.W. Rubel (1978) Ontogeny of behavioral responsiveness to sound in the chick embryo as indicated by electrical recordings of motility. J. Comp. Physiol. Psychol. *92:*682–696.

Jeffress, L.A. (1948) A place theory of sound localization. J. Comp. Physiol. Psychol. *41:*35–39.

Jeffress, L.A. (1975) Localization of sound. Chapter 10. In W.D. Keidel and W.D. Neff (eds): Handbook of Sensory Physiology, Vol V, Part 2, Auditory System. New York: Springer-Verlag. pp 449–459.

Jhaveri, S., and D.K. Morest (1982a) Neuronal architecture in nucleus magnocellularis of the chicken auditory system with observations on nucleus laminaris: A light and electron microscope study. Neuroscience *7:*809–836.

Jhaveri, S., and D.K. Morest (1982b) Sequential alterations of neuronal architecture in nucleus magnocellularis of the developing chicken: A golgi study. Neuroscience *7:*837–853.

Jhaveri, S., and D.K. Morest (1982c) Sequential alterations of neuronal

architecture in nucleus magnocellularis of the developing chicken: An electron microscope study. Neuroscience 7:855–870.

Johnson, D.A., and D. Purves (1981) Post-natal reduction of neural unit size in the rabbit ciliary ganglion. J. Physiol. (Lond.) *318:*143–159.

Keshishian, H., and D. Bentley (1983a) Embryogenesis of peripheral nerve pathways in grasshopper legs. I. The initial nerve pathway to the CNS. Dev. Biol. *96:*89–102.

Keshishian, H., and D. Bentley (1983b) Embryogenesis of peripheral nerve pathways in grasshopper legs. II. The major nerve routes. Dev. Biol. *96:*103–115.

Keshishian, H., and D. Bentley (1983c) Embryogenesis of peripheral nerve pathways in grasshopper legs. III. Development without pioneer neurons. Dev. Biol. *96:*116–124.

Knudsen, E.I. (1985) Experience alters the spatial tuning of auditory units in the optic tectum during a sensitive period in the barn owl. J. Neurosci. *5:*3094–3109.

Lance-Jones, C., and L. Landmesser (1980) Motoneurone projection patterns in the chick hind limb following early partial reversals of the spinal cord. J. Physiol. *302:*581–602.

Landmesser, L. (1978) The development of motor projection patterns in the chick hind limb. J. Physiol. *284:*391–414.

Law, M.I., and M. Constantine-Paton (1981) Anatomy and physiology of experimentally produced striped tecta. J. Neurosci. *1:*741–759.

LeVay, S., D.H. Hubel, and T.N. Wiesel (1975) The pattern of ocular dominance columns in macaque visual cortex revealed by a reduced silver stain. J. Comp. Neurol. *159:*559–576.

LeVay, S., M.P. Stryker, and C.J. Shatz (1978) Ocular dominance columns and their development in Layer IV of the cat's visual cortex: A quantitative study. J. Comp. Neurol. *179:*223–244.

Lichtman, J.W. (1977) The reorganization of synaptic connections in the rat submandibular ganglion during post-natal development. J. Physiol. (Lond.) *273:*155–177.

Lichtman, J.W., and D. Purves (1980) The elimination of redundant preganglionic innervation to hamster sympathetic ganglion cells in early postnatal life. J. Physiol. (Lond.) *301:*213–228.

Lippe, W., and E.W. Rubel (185) Ontogeny of tonotopic organization of brain stem auditory nuclei in the chicken: Implications for development of the place principle. J. Comp. Neurol. *273:*273–289.

Mason, C.A. (1982) Development of terminal arbors of retinogeniculate axons in the kitten—I. Light microscopical observations. Neuroscience 7:541–559.

Mason, C.A. (1985) Growing tips of embryonic cerebellar axons in vivo. J. Neurosci. *13:*55–73.

Mason, C.A., and E. Gregory (1984) Postnatal maturation of cerebellar mossy and climbing fibers: Transient expression of dual features on single axons. J. Neurosci. *4:*1715–1735.

McLoon, S.C. (1985) Evidence for shifting connections during development of the chick retinotectal projection. J. Neurosci. *5:*2570–2580.

Metcalfe, W.K. (1985) Sensory neuron growth cones comigrate with posterior lateral line primordial cells in zebrafish. J. Comp. Neurol. *238:*218–224.

Meyer, R.L. (1983) The growth and formation of ocular dominance columns by deflected optic fibers in goldfish. Dev. Brain. Res. *6:*279–291.

Moiseff, A., and M. Konishi (1983) Binaural characteristics of units in the owl's brainstem auditory pathway: Precursors of restricted spatial receptive fields. J. Neurosci. *3:*2553–2562.

Morest, D.K. (1968) The growth of synaptic endings in the mammalian brain: A study of the calyces of the trapezoid body. Z. Anat. Entwickl.-Gesch. *127:*201–220.

Morest, D.K. (1969) The differentiation of cerebral dendrites: A study of post-migratory neuroblast in the medial nucleus of the trapezoid body. Z. Anat. Entwickl.-Gesch. *128:*271–289.

Morest, D.K. (1970) A study of neurogenesis in the forebrain of opossum pouch young. Z. Anat. Entwickl.-Gesch. *130:*265–305.

Parks, T.N. (1979) Afferent influences on the development of the brain stem auditory nuclei of the chicken: Otocyst ablation. J. Comp. Neurol. *183:*665–678.

Parks, T.N. (1981) Morphology and origin of axosomatic endings in an avian cochlear nucleus: Nucleus magnocellularis of the chicken. J. Comp. Neurol. *203:*425–440.

Parks, T.N., P. Collins, and J.W. Conlee (1983) Morphology and origin of axonal endings in nucleus laminaris of the chicken. J. Comp. Neurol. *214:*32–42.

Parks, T.N., and H. Jackson (1984) A developmental gradient of dendritic loss in the avian cochlear nucleus occurring independently of primary afferents. J. Comp. Neurol. *227:*459–466.

Parks, T.N., and E.W. Rubel (1975) Organization and development of brain stem auditory nuclei of the chicken: Organization of projection from N. magnocellularis to N. laminaris. J. Comp. Neurol. *164:*435–448.

Purves, D., and J.W. Lichtman (1985) Principles of Neural Development. Sunderland, MA: Sinauer.

Purves, D., W. Thompson, and J.W. Yip (1981) Re-innervation of ganglia transplanted to the neck from different levels of the guinea-pig sympathetic chain. J. Physiol. (Lond.) *313:*49–63.

Rakic, P. (1972) Mode of cell migration to the superficial layers of fetal monkey neocortex. J. Comp. Neurol. *145:*61–84.

Rakic, P. (1977a) Genesis of the dorsal lateral geniculate nucleus in the rhesus monkey: Site and time of origin, kinetics of proliferation, routes of migration and pattern of distribution of neurons. J. Comp. Neurol. *176:*23–52.

Rakic, P. (1977b) Prenatal development of the visual system in Rhesus monkey. Philos. Trans. R. Soc. Lond. [Biol.] *278:*245–260.

Rakic, P. (1981) Development of visual centers in the primate brain depends on binocular competition before birth. Science *214:*928–931.

Ramón y Cajal, S. (1960) Studies on Vertebrate Neurogenesis (Translated by L. Guth). Springfield, IL: Thomas.

Raper, J.A., M. Bastiani, and C.S. Goodman (1983a) Pathfinding by neuronal growth cones in grasshopper embryos. I. Divergent choices made by the growth cones of sibling neurons. J. Neurosci. *3:*20–30.

Raper, J.A., M. Bastiani, and C.S. Goodman (1983b) Pathfinding by neuronal growth cones in grasshopper embryos. II. Selective fasciculation onto specific axonal pathways. J. Neurosci. *3:*31–41.

Rebillard, G., and E.W. Rubel (1981) Electrophysiological study of the maturation of auditory respones from the inner ear of the chick. Brain. Res. *229:*15–23.

Redfern, P.A. (1970) Neuromuscular transmission in new-born rats. J. Physiol. (Lond.) *209:*701–709.

Reh, T.A., and M. Constantine-Paton (1984) Retinal ganglion cell terminals change their projection sites during larval development of Rana pipiens. J. Neurosci. *4:*442–457.

Reh, T.A., and M. Constantine-Paton (1985) Eye-specific segregation requires neural activity in three-eyed Rana pipiens. J. Neurosci. *5:*1132–1143.

Reh, T.A., E. Pitts, and M. Constantine-Paton (1983) The organization of the fibers in the optic nerve of normal and tectum-less Rana pipiens. J. Comp. Neurol. *218:*282–296.

Ross, C.D., and D.A. Godfrey (1984) Choline acetyltransferase (ChAT) activity in layers of goldfish optic tectum following eye removal. Soc. Neurosci. Abstr. *170:*6.

Rubel, E.W., and T.N. Parks (1975) Organization and development of brain stem auditory nuclei of the chicken: Tonotopic organization of N. magnocellularis and N. laminaris. J. Comp. Neurol. *164:*411–434.

Rubel, E.W., D.J. Smith, and L.C. Miller (1976) Organization and development of brain stem auditory nuclei of the chicken: Ontogeny of N. magnocellularis and N. laminaris. J. Comp. Neurol. *166:*469–490.

Rubel, E.W., Z.D.J. Smith, and O. Steward (1981) Sprouting in the avian brain stem auditory pathway: Dependence on dendritic integrity. J. Comp. Neurol. *202:*397–414.

Rubin, E. (1985a) Development of the rat superior cervical ganglion: Ingrowth of preganglionic axons. J. Neurosci. *5:*685–696.

Rubin, E. (1985b) Development of the rat superior cervical ganglion: Initial stages of synapse formation. J. Neurosci. *5:*697–704.

Sakaguchi, D.S., and R.K. Murphey (1985) Map formation in the developing Xenopus retinotectal system: An examination of ganglion cell terminal arborizations. J. Neurosci. *5:*3228–3245.

Sanes, D.H., and M. Constantine-Paton (1985) The sharpening of frequency tuning curves requires patterned activity during development in the mouse, Mus musculus. J. Neurosci. *5:*1152–1166.

Saunders, J.C., R.B. Coles, and G.R. Gates (1973) The development of auditory evoked responses in the cochlear and cochlear nuclei of the chick. Brain. Res. *63:*59–74.

Schmidt, J.T. (1985) Apparent movement of optic terminals out of a local post-synaptically blocked region in goldfish optic tectum. J. Neurophysiol. *53:*237–251.

Shatz, C.J., and P.A. Kirkwood (1984) Prenatal development of functional connections in the cat's retino-geniculate pathway. J. Neurosci. *4:*1378–1397.

Shatz, C.J., and M.P. Stryker (1978) Ocular dominance in layer IV of the

cat's visual cortex and the effects of monocular deprivation. J. Physiol. (Lond.) *281:*267–283.

Smith, Z.D.J. (1981) Organization and development of brain stem auditory nuclei of the chicken: dendritic development of N. laminaris. J. Comp. Neurol. *203:*309–333.

Smith, D.J., and E.W. Rubel (1979) Organization and development of brain stem auditory nuclei of the chicken: Dendritic gradients in nucleus laminaris. J. Comp. Neurol. *186:*213–240.

Smolen, A., and G. Raisman (1980) Synapse formation in the rat superior cervical ganglion during normal development and after neonatal deafferentation. Brain. Res. *181:*315–323.

Sretavan, D., and C.J. Shatz (1986) Prenatal development of retinal ganglion cell axons: Segregation into eye-specific layers within the cat's lateral geniculate nucleus. J. Neurosci. *6:*234–251.

Srihari, T., and G. Vrbova (1978) The role of muscle activity in the differentiation of neuromuscular junctions in slow and fast chick muscles. J. Neurocytol. *7:*529–540.

Stent, G.S. (1973) A physiological mechanism for Hebb's postulate of learning. Proc. Natl. Acad. Sci. USA *70:*997–1001.

Stryker, M.P. (1981) Late segregation of geniculate afferents to the cat's visual cortex after recovery from binocular impulse blockade. Soc. Neurosci. Abstr. *7:*842.

Stryker, M.P. (1982) Role of visual afferent activity in the development of ocular dominance columns. Neurosci. Res. Progr. Bull. *20:*540–549.

Stryker, M.P., and W.A. Harris (1986) Binocular impulse blockade prevents the formation of ocular dominance columns in cat visual cortex. J. Neurosci. *6:*2117–2133.

Stuermer, C.A.O., and S.S. Easter (1984) Rules of order in the reinotectal fascicles of goldfish. J. Neurosci. *4:*1045–1051.

Tosney, K.W., and L.T. Landmesser (1984) Pattern and specificity of axonal outgrowth following varying degrees of chick limb bud ablation. J. Neurosci. *4:*2515–2527.

Tosney, K.W., and L.T. Landmesser (1985a) Specificity of early motoneuron growth cone outgrowth in the chick embryo. J. Neurosci. *5:*2336–2344.

Tosney, K.W., and L.T. Landmesser (1985b) Growth cone morphology and trajectory in the lumbosacral region of the chick embryo. J. Neurosci. *5:*2345–2358.

Tumosa, N., W.K. Stell, and F. Eckenstein (1984) Choline acetyltransferase immunoreactivity is located in intrinsic neurons but not in retinal afferent terminals in the goldfish tectum. Soc. Neurosci. Abstr. *170:*7.

Udin, S.B. (1984) The morphology of isthmo-tectal axon arbors in developing *Xenopus* frogs. Soc. Neurosci. Abstr. *301:*1.

Wallace, B.G. (1984) Selective loss of neurites during differentiation of cells in the leech central nervous sytem. J. Comp. Neurol. *228:*149–153.

Wigston, D.J., and J.R. Sanes (1982) Selective reinnervation of adult mammalian muscle by axons from different segmental levels. Nature *229:*464–467.

Winer, B.J. (1971) Statistical Principles in Experimental Design, 2nd Ed. New York: McGraw-Hill.

Young, S.R. (1985) The development of the projections from nucleus magnocellularis to nucleus laminaris in the chick brain stem: An HRP study of individual axon terminal arborizations in a topographically organized auditory nucleus. Doctoral dissertation, University of Virginia.

Young, S.R., and E.W. Rubel (1983) Frequency specific projections of individual neurons in chick brain stem auditory nuclei. J. Neurosci. *3:*1373–1378.

Young, S.R., and E.W. Rubel (1984) The embryonic development of axonal arborizations in nucleus laminaris of the chick auditory system. Soc. Neurosci. Abstr. *16:*20.